Environmental enrichment and physical exercise prevent stress-induced behavioral and blood-brain barrier alterations *via* Fgf2.

Sam E.J. Paton[1], José L. Solano[1], Adeline Collignon[1], Émanuelle Richer[1], François Coulombe-Rozon[1], Laurence Dion-Albert[1], Luisa Bandeira Binder[1], Katarzyna Anna Dudek[1], Alice Cadoret[1], Signature Consortium[2], Manon Lebel[1], Caroline Ménard[1]

[1]Department of Psychiatry and Neuroscience, Faculty of Medicine and CERVO Brain Research Center, Université Laval, Quebec City, QC, Canada
[2]Institut universitaire en santé mentale de Montréal, Centre intégré universitaire de santé et service sociaux Est, Montreal, QC, Canada

Number of pages: 46
Number of figures: 6 (+6 supplementary figures)
Number of tables: 0 (+3 supplementary tables)
Number of words: 6,060 for the main text

§**Corresponding author**:

Caroline Menard, PhD
CERVO Brain Research Center
Department of Psychiatry and Neuroscience
Faculty of Medicine, Université Laval
2601 de la Canardiere
Quebec City, QC, Canada G2J 2G3
(418) 663-5741
E-mail: caroline.menard@fmed.ulaval.ca

Running title: Preventive strategies for stress-induced neurovascular alterations

Keywords: Resilience, depression, preventive strategies, inflammation, growth factor, endothelial cells

Summary

Chronic stress can promote loss of blood-brain barrier (BBB) integrity leading to passage of circulating inflammatory mediators in mood-regulating brain areas and establishment of depressive behaviors. Conversely, neurovascular adaptations favoring resilience to stress exposure remain undetermined. Here, we report that environmental enrichment dampens stress-induced loss of endothelial tight junction protein Claudin-5 (Cldn5) along with anxiety- and depression-like behaviors in mice via an increase in fibroblast growth factor 2 (Fgf2). Treatment of mouse and human endothelial cells with Fgf2 preceding an immune challenge with the proinflammatory cytokine TNFα, elevated after chronic stress and in depression, reduces BBB dysfunction, and altered cell signaling. Coping with voluntary physical exercise also protects the BBB from stress deleterious effects by increasing Fgf2 preventing Cldn5 loss, exacerbated inflammation, and social avoidance. Circulating FGF2 level is linked with depression severity and symptomatology in humans supporting involvement of this growth factor in mood disorders and stress-induced BBB changes.

Introduction

Major depressive disorder (MDD) is a psychiatric condition affecting >300 million people worldwide, representing a growing burden on global health systems[1]. Common antidepressants are largely ineffective with 30-50% of individuals with MDD poorly responding to existing therapies, suggesting that underlying causal mechanisms remain unaddressed[2,3]. Women are twice as likely to be diagnosed with depression, and MDD presents sex differences in symptoms, treatment responses, and brain transcriptional profiles[4-7]. Women also report higher levels of chronic stress, a major environmental risk factor for development of depression, which promotes neurovascular pathology by damaging the blood-brain barrier (BBB) in preclinical models and human MDD samples[3,8-11]. Specifically, chronic stress is associated with a sustained elevation of circulating inflammatory mediators, activation of brain endothelial cells via elevated cytokine expression, leukocyte adhesion, and degradation of tight junction protein Claudin-5 (Cldn5) leading to increased barrier permeability[9,11,12]. The BBB is a physical frontier mediating communication between the periphery and the brain, composed of an intricate cellular network including astrocytes, pericytes, and endothelial cells connected by specialized tight junctions[3,13]. This distinctive composition enables metabolic supply while also ensuring a selective permeability which protects the brain from bloodstream harmful toxins and inflammatory factors[14,15]. Consequently, the BBB is necessary to maintain normal neural activity, and disruption can lead to neuroinflammation, neuronal death, and severe cognitive deficits[3]. BBB alterations and tight junction loss have been observed in individuals with MDD, as well as mice subject to chronic stress, in a sex- and brain region-specific manner[8,9,16,17]. Interestingly, in other mental conditions like bipolar disorder and schizophrenia the degree of BBB damage appears to correlate with age of onset as well as disease severity[18,19], suggesting that the neurovasculature could represent an innovative target for effective intervention against mood disorder development and progression.

Environmental conditions which promote stress resilience and neurovascular health offer a promising approach to identify novel therapeutic sites. Indeed, stimulating environments are well known to positively alter the adult brain including vascularization and BBB function[20-23]. Further, circumstantial factors such as socioeconomic status and physical activity are negatively correlated with depression risk in humans[24,25], while in mice, access to nesting material, shelter, and toys (enriched environment, EE) or a running wheel (physical exercise, PE) attenuates depression-like behaviors following stress exposure[26,27]. Involvement of the BBB in these outcomes has not yet been assessed; however, we recently observed neurovascular changes after learning and memory tasks depending on environmental conditions[28]. The present study expands this idea by combining behavioral studies performed in male and female mice with *in vitro* cell signaling work to identify functional and transcriptional adaptations of the BBB involved in the pro-resilient effects of EE and PE during chronic stress. We show that environmental intervention can rescue stress-induced deficits in social behavior and expression of tight junction proteins Cldn5 in both sexes. Further, we identify fibroblast growth factor 2 (Fgf2) as a protective factor upregulated in response to stress in the nucleus accumbens (NAc) of males with access to either EE or voluntary PE. The NAc is a hub for mood regulation, reward, and stress responses[29]. Fgf2 can prevent inflammatory activation of brain endothelial cells, as well as subsequent loss of barrier integrity by increasing Cldn5 expression, suggesting a potential protective mechanism. Finally, we associate a change in

circulating Fgf2 with depressive symptoms in human cohorts and highlight sex differences as well as the impact of university education, an important indicator of socioeconomic status.

Results

Environmental enrichment dampens stress-induced social avoidance and blood-brain barrier alterations in male mice.

The standard chronic social defeat stress (CSDS) protocol, a commonly used mouse model of depression in which C57Bl/6 are exposed daily (5 min/day) for 10 days to a physical bout with an aggressive CD-1 mice, places animals in a plastic cage with no supplements such as toys, shelter, or nesting material[9]. In these conditions, about two-thirds of stressed mice display social avoidance and are classified as stress-susceptible (SS) while the other third, showing no behavioral deficits, are considered resilient (RES)[9,30]. However, compared to wild mice this is a reductive setting, and introducing a more stimulating environment has been shown to improve the behavioral response to CSDS[26]. To evaluate if environmental enrichment (EE) has an impact on stress-induced BBB alterations, male C57Bl/6 were given access to nesting material, a shelter, and plastic chew toy on their side of the CSDS cage throughout the stress paradigm (**Fig.1A**). As expected, the EE increased the proportion of mice classified as resilient to more than half (57.9%) along with the SI ratio of stressed mice when compared to standard CSDS (**Fig.1B**, stress x environment effect: $^{**}p=0.0029$). Importantly, stressed EE mice spent similar time in the corners during the SI test compared to unstressed controls while mice subjected to CSDS in a standard environment developed social avoidance (**Fig.1C** and **Supp.Fig.1A**, $^{****}p<0.0001$).

To probe a role for the BBB in these positive effects, we next investigated stress-induced changes for transcription of BBB-related genes involved in cell proliferation, vascular remodeling, tight junction formation, or markers of astrocyte, pericyte, and neuroinflammation, in the nucleus accumbens (NAc) and prefrontal cortex (PFC), two brain regions involved in the onset of depressive-like behaviors in mice and MDD in humans (**Fig.1D** and **Supp.Fig.1B** for behavioral data). Standard CSDS reduces the expression of *Cldn5*, a key tight junction protein, specifically in the male NAc, and increases expression of inflammatory cytokine interleukin-6 (*Il-6*)[9]. In contrast, we found in the NAc of stressed EE mice a general increase in gene expression associated with vascular remodeling and tight junction formation relative to unstressed EE control, including for *Cldn5* (**Fig.1D**, left, $^{*}p=0.0253$), as well as growth factors, particularly *Fgf2* ($^{*}p=0.038$) which is linked to BBB integrity[31,32] and antidepressant behavioral effects[33-37]. No change in *Cldn5* was observed in the male PFC in line with intact BBB integrity[9], but expression of several growth factors including *Fgf2* was upregulated (**Fig.1D**, right, $^{*}p=0.0196$), suggesting adaptive mechanisms. Comparison of NAc gene expression from standard CSDS and EE cohorts indicates a beneficial effect of EE through prevention of both *Cldn5* loss (**Fig.1E**, $^{****}p<0.0001$) and increased inflammatory *Il-6* ($^{*}p=0.0318$) following CSDS. Previous reports from standard CSDS show that SS and RES mice display substantially different transcriptional patterns[38]. Principal component analysis (PCA) on the gene transcripts in our EE cohort revealed that SS and RES mice strongly overlap (**Fig.1F**). Indeed, when comparing gene expression patterns from our EE mice

with previously published standard environment CSDS[9], and our EE mice, we found evidence for close clustering of all behavioral phenotypes (CTRL, SS, and RES) based on BBB-related gene expression, in EE but not standard housed CSDS cohorts (**Fig.1F** and **Supp.Fig.1F**).

To confirm gene expression changes at protein level, immunofluorescent staining was performed to label for Cldn5, Fgf2, and Cd31, a marker of blood vessels, in brain slices from the NAc and PFC of unstressed control, SS and RES mice (**Fig.1G** and **Supp.Fig.1C** for behavioral data). In standard CSDS, Cldn5 coverage of blood vessels is reduced by ~50% in the NAc of SS male mice[9]. With EE, this loss is dampened supporting compensatory changes (**Fig.1G**, **Supp.Fig.1D** for Cd31). In this line, while chronic stress has been reported to reduce *Fgf2* expression in a standard environment in the PFC[39], stressed mice in our EE cohort had increased Fgf2 in the NAc (*p=0.0472), and this tend to correlate with the degree of Cldn5 loss (r=-0.4882, p=0.0648) (**Fig.1G**). No change was observed in the PFC in EE conditions (**Supp.Fig.1E**). Altogether, our findings suggest that access to an enriched environment has a protective effect on stress-induced BBB alterations via Fgf2.

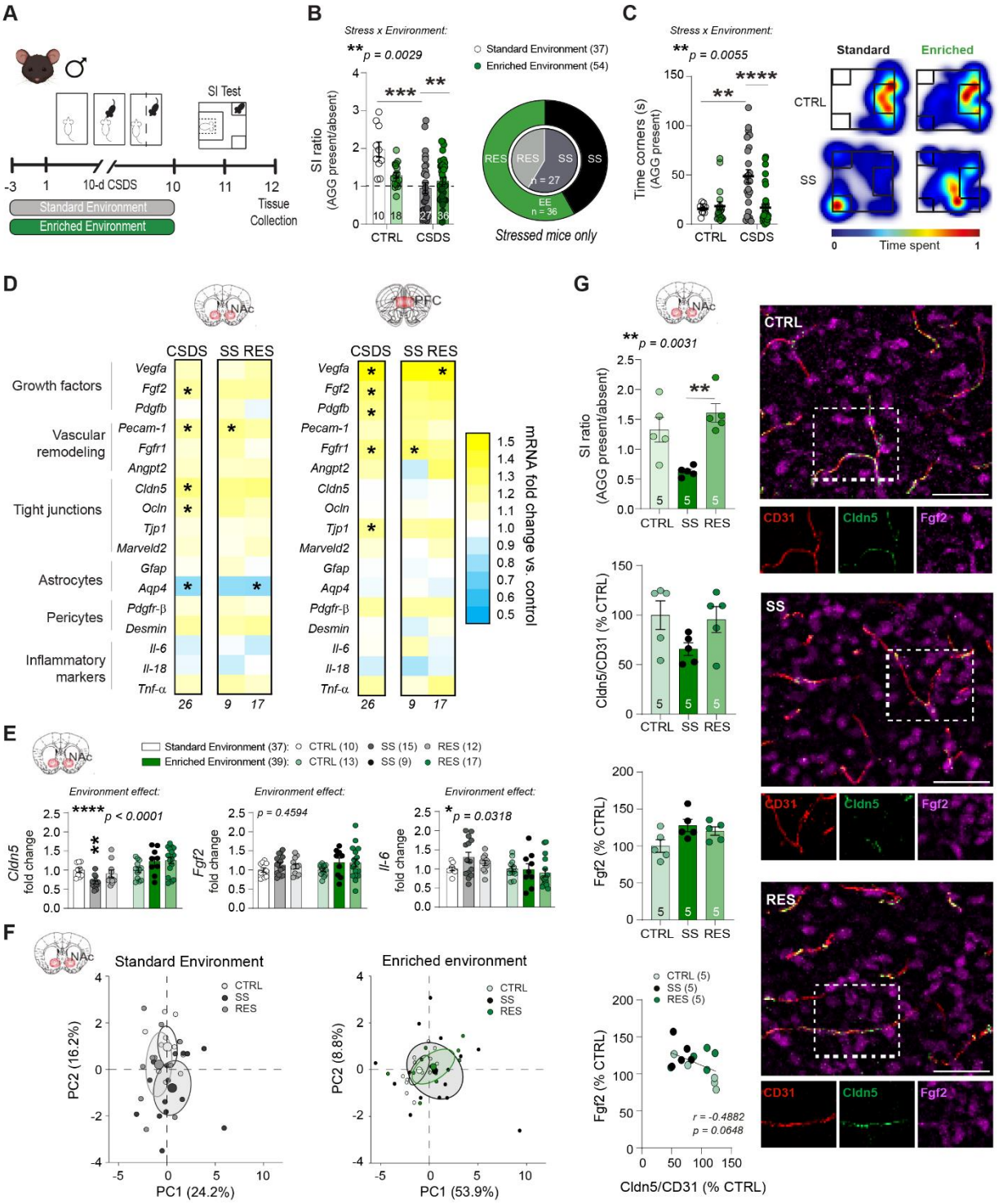

Figure 1. Environmental enrichment dampens stress-induced social avoidance and blood-brain barrier alterations in male mice. A, Experimental timeline for chronic social defeat stress (CSDS) with enriched environment (EE). Male mice were housed with a nestlet, plastic chew toy, and shelter beginning 3 d prior to CSDS and continuing until the last defeat, followed by social interaction (SI) testing. **B,** Compared to previously published results from CSDS with standard cages[9], stressed EE mice show less deficits in social behavior measured by the SI test, and a greater percentage of resilience. **C,** Stressed EE mice also show less time in corners of the SI test than those stressed in plain cages. Representative heatmaps of SI test in the second trial (aggressor present) show differences between

CTRL and SS mice in CSDS with standard caging[9] and EE. **D,** Heatmap showing transcription of BBB-related genes in the nucleus accumbens (NAc) and prefrontal cortex (PFC) after stress for EE mice. Cldn5, Ocln, and Fgf2 are upregulated in the NAc of all stressed mice. **E,** Increased Cldn5 expression and decreased Il-6 in SS EE mice compared to published data from SS mice in plain cages[9]. **F,** CTRL, SS, and RES behavioral groups form distinct clusters based on principal component analysis of NAc gene expression data in standard CSDS but are grouped together in EE. **G,** Fgf2 immunofluorescent labelling is increased in all stressed mice from the EE cohort while Cldn5 relative to blood vessel area is diminished specifically in SS mice (scalebar = 50 μm). Fgf2 area correlates with degree of Cldn5 loss suggesting a protective response. Data represent mean ± s.e.m., the number of animals is indicated on graphs. Group comparisons were evaluated with one- or two-way ANOVA followed by Bonferroni's post hoc tests and correlation with Pearson's correlation coefficient or t-tests with Welch's correction where appropriate; *p<0.05, **p<0.01, ***p<0.001, ****p<0.0001.

Environmental enrichment rescues stress-related transcriptomic deficits in female mice.

While CSDS is a standard protocol to induce social stress in male mice, it is not as relevant for female mice who do not commonly experience aggression in the wild[40]. Artificial methods for inducing social defeat in females exist, including application of male urine to promote aggressive bouts[41], but it introduces sensory information which may interfere with enrichment effects. In our hands still only ~30% of female mice become susceptible to 10-day CSDS with this protocol, hampering the possibility to test preventive or protective approaches[8]. Thus, to evaluate whether EE could promote resilience in females, we took advantage of the subchronic variable stress (SCVS) paradigm, an established protocol producing anxiety and anhedonia after 6 days[8,42] along with BBB changes in the PFC[8]. Female mice assigned to control or SCVS groups had access to EE as described above and the SCVS group was exposed to a series of three repeated stressors, namely foot shock, tail suspension, and tube restraint (**Fig.2A**). Following SCVS, a cohort was subjected to a battery of behavioral tests to assess the impact of EE on stress responses (**Supp.Fig.2A**). Compared to 6-d SCVS with standard housing[8], access to EE prevented stress-induced reduction in time spent in the elevated plus maze (EPM) open arms (**Fig.2B**, ***p=0.0002), increased social interactions (*p=0.0297), and sucrose preference (****p<0.0001) (**Supp.Fig.2B-F**). A 2nd cohort of EE mice was tested in the EPM only to confirm normal behaviors despite stress exposure, then brain tissue was collected 24h later (**Fig.2A** and **Supp.Fig.3A, D** for behavioral data) so 48h after the last stressor like for males (**Fig.1A**). No difference in estrous cycle stage was observed between CTRL and SCVS groups at tissue collection (**Supp.Fig.3B**).

Neurovascular disruption in the PFC underlies the development of anxiety- and depression-like behaviors in female mice and a loss of CLDN5 was noted in this brain area in postmortem samples from women with MDD[8]. Gene expression analysis showed that EE stabilizes BBB transcriptomic patterns in the PFC (**Fig.2C**), leading to maintenance of *Cldn5* expression vs SCVS in standard housing (**Fig.2D**, **p=0.0024) and normal behaviors despite stress exposure. Next, BBB-related gene expression patterns in the female PFC were compared after SCVS in standard vs EE conditions with PCA analysis. We revealed that with standard housing, CTRL and SCVS mice form distinct clusters, while with EE they are more closely grouped (**Fig.2E**). Because EE reduces transcriptional differences between control and stressed mice in both males and females, gene expression patterns were compared in the NAc and PFC across sexes. Even if the behavioral outcomes are similar, BBB-related transcriptomic profiles of males and females differ, suggesting that environmental influence on the neurovasculature is sex-specific (**Fig.2F**, **Supp.Fig.3F-G**). Given the implication of Fgf2 as a protective factor in males, we assessed its protein level along

with Cldn5 and Cd31 in females. Immunofluorescent staining confirmed an absence of stress-induced changes in Cldn5 but also Fgf2 in both PFC (**Fig.2G)** and NAc (**Supp.Fig.3C-E)** in the female EE cohort. These results suggest that females benefit from an EE however, elevation of Fgf2 might be a male specific protective mechanism for pro-resilient effects on the BBB.

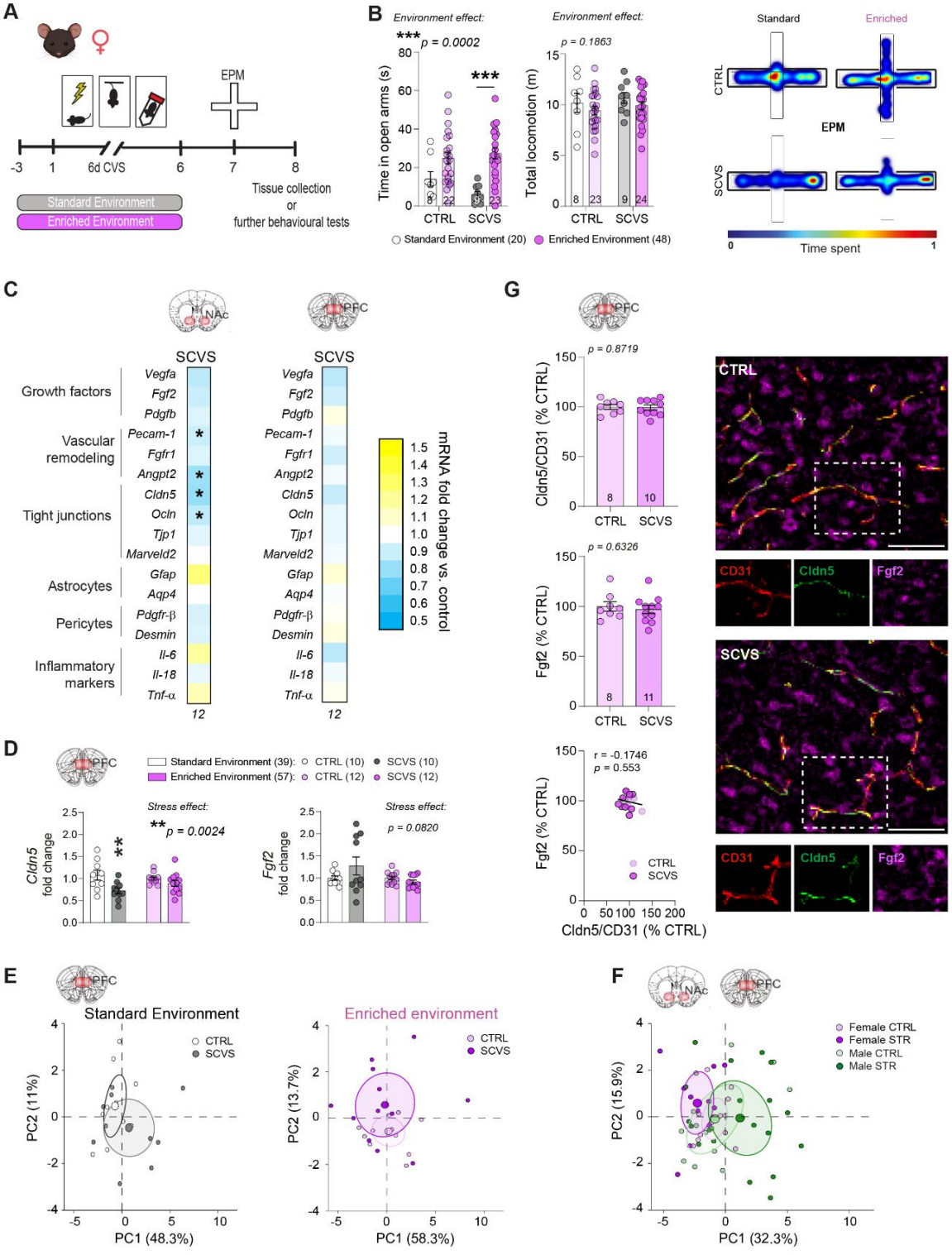

Figure 2. Environmental enrichment dampens stress-induced anxiety and blood-brain barrier alterations in the prefrontal cortex of female mice. A, Experimental timeline for subchronic variable stress (SCVS) with enriched environment (EE). Female mice were housed with a nestlet, plastic chew toy, and shelter beginning 3 days prior to stress and continuing until the last session, followed by elevated plus maze (EPM). **B,** Compared to previously published results from female SCVS with plain cages[8], stressed EE mice show greater exploratory behavior characterized by open arm time in the EPM. Representative heatmaps show differences in EPM behavior between standard and EE SCVS. **C,** Heatmaps showing transcription of BBB-related genes in the nucleus accumbens (NAc) and prefrontal cortex (PFC) after stress. Cldn5 deficits are seen in the NAc, but not the PFC. **D,** Increased Cldn5 expression in stressed EE mice compared to published data from stressed mice in plain cages[8]. **E,** CTRL and SCVS mice form distinct clusters based on principal component analysis of PFC gene expression data when performed in standard cages, but in the EE cohort they are more closely grouped. **F,** BBB-related genes in the male NAc and female PFC respond differently to stress. **G,** No changes in immunofluorescent staining of Fgf2 or Cldn5 following SCVS in female mice with EE (scalebar = 50 μm). Data represent mean ± s.e.m., the number of animals is indicated on graphs. Group comparisons were evaluated with two-way ANOVA followed by Bonferroni's post hoc tests or t-tests with Welch's correction; *p<0.05, **p<0.01, ***p<0.001.

In vitro treatment with Fgf2 reduces TNF-α-induced Cldn5 loss, endothelial cell signaling alterations, and barrier hyperpermeability.

BBB disruption is associated with stress-induced behavioral deficits in mice[8-11] and psychiatric disorders including MDD in humans[8,9,18,19,38,43]. Fgf2 can mediate formation of tight junctions in endothelial cells[31,32], nevertheless it is undetermined if Fgf2 could protect against stress-related neurovascular damage. Our findings indicate a role for Fgf2 in protective effects of EE on the NAc BBB, specifically in male mice, with upregulation of this growth factor occurring in parallel with increased Cldn5 expression at both gene and protein level in stressed mice with access to EE (**Fig.1**). Therefore, we investigated whether Fgf2 can preserve brain endothelial cell properties *in vitro* using treatment with the proinflammatory cytokine TNF-α as a biological stressor. Indeed, TNF-α is elevated in the blood of mice after CSDS and individuals with MDD[44-46], while downstream signaling through TNF receptors is linked to stress-induced BBB breakdown in mice[10,38]. To ensure translational relevance we exposed both human (HBEC-5i) and mouse (bEnd.3) brain endothelial cell lines to either acute (<24h) or chronic (up to 7 days) periods of inflammatory challenge with 10 ng/mL of TNF-α (**Fig.3A**). Cells were pretreated for 1h with FGF2 to mimic habituation with EE, before co-stimulation with TNF-α and/or FGF2. Following TNF-α treatment, expression of genes associated with tight junctions, FGF2 signaling, and proinflammatory activation of endothelial cells was evaluated at several timepoints (1, 3, 6 or 24h). Acute TNF-α stimulation induced strong endothelial cell activation characterized by downregulation of tight junction proteins *CLDN5* and *OCLN*, as well as expression of inflammatory factors such as *IL-6* (HBEC-5i) and *Vcam-1* (bEnd.3) (**Fig.3B-C**). In both cell types, FGF2 attenuated TNF-α-induced loss of *CLDN5*, with protective effects especially prominent after 6h of treatment (**Fig.3D-E**, *p=0.0119 for mouse and ***p=0.0004 for human endothelial cells).

Since FGF2 could reverse the effects of acute TNF-α treatment on *CLDN5* expression we next tested if it could prevent loss in barrier integrity following long-term TNF-α exposure. Chronic stimulation with TNF-α over 7 days altered endothelial monolayer integrity as measured with transendothelial electrical resistance (TEER) when compared to control wells, by day 1 in bEnd.3 and day 3 in HBEC-5i, and this effect was prevented by FGF2 co-treatment (**Fig.3F-G**, **p=0.0014 for mouse and ****p<0.0001 for human endothelial cells). FGF2 is a potent mitogen

thus, an MTT assay was conducted to rule out potential changes in cell number which could influence TEER. Once confluent, FGF2 did not influence cell number vs controls (**Supp.Fig.4**). On day 7 of the TEER protocol, cells were fixed and stained for Cldn5 to visualize tight junctions. bEnd.3 cells treated with TNF-α showed disruption of tight junction structure including presence of spikes, discontinuities, and membrane ruffling which are signs of endothelial dysfunction[47]; however, this morphology was not observed for cells co-stimulated with Fgf2 (**Fig.3H**).

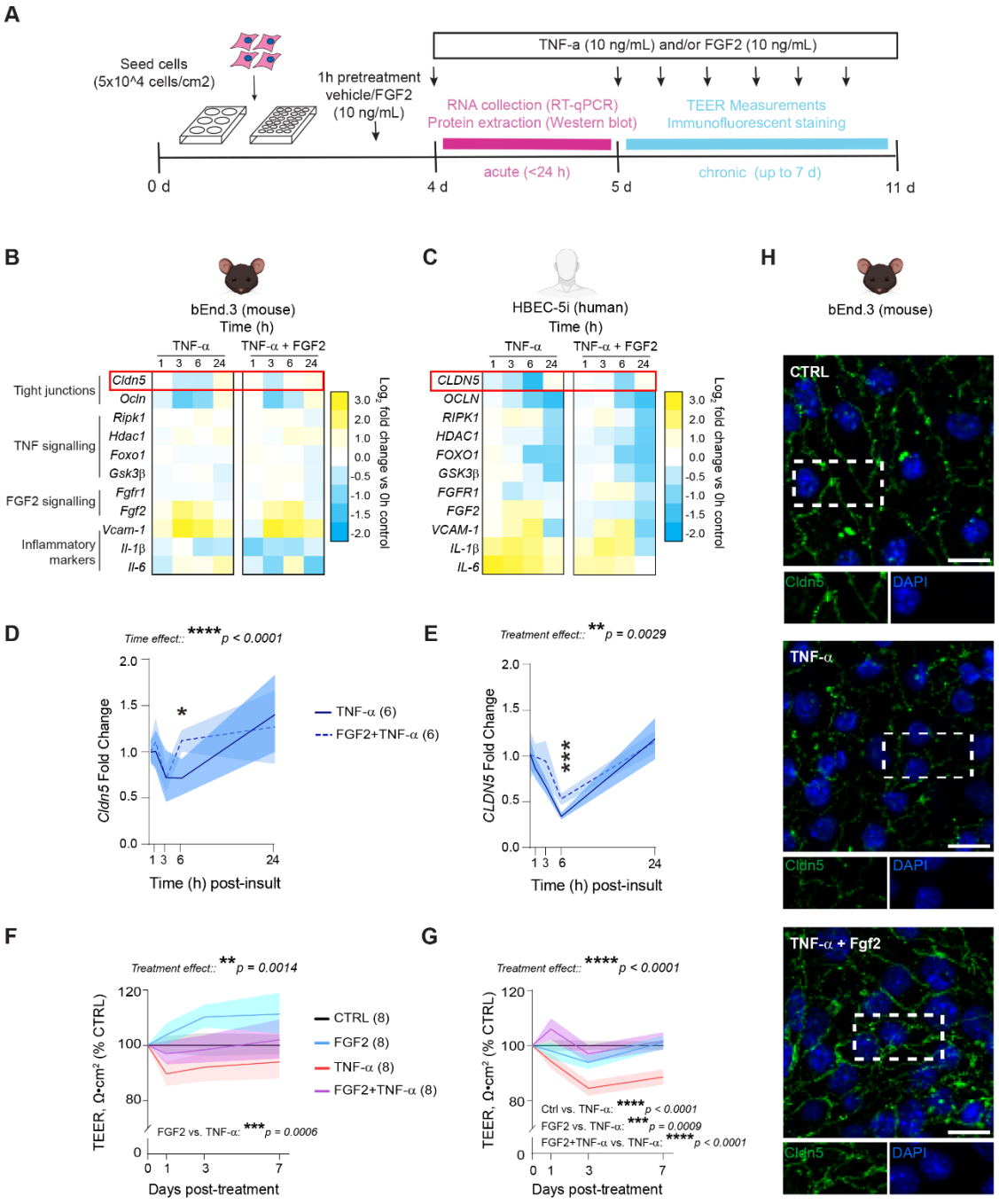

Figure 3. Treatment with Fgf2 reduces TNF-α-induced Cldn5 loss, endothelial cell signaling alterations, and barrier hyperpermeability. A, Experimental timeline for inflammatory insult with TNF-α and FGF2 co-treatment.

Once confluent (4 days), HBEC-5i or bEnd.3 were pretreated with FGF2 or vehicle for one hour and then stimulated with TNF-α or vehicle for up to 7 days. FGF2 alters mouse (**B**) and human (**C**) endothelial transcription in response to acute TNF-α stimulation. FGF2 promotes faster restoration of TNF-α -induced Cldn5 loss in mouse (**D**) and human (**E**) endothelial cells. **F, G** Chronic stimulation with TNF-α leads to a reduction in endothelial monolayer integrity measured by trans-endothelial electrical resistance (TEER). FGF2 co-treatment preserves normal TEER despite TNF-α. **H,** 7 days of TNF-α treatment promotes spikes and discontinuities in Cldn5 tight junction strands in bEnd.3, which is reversed by FGF2 treatment (scalebar = 20 μm). Data represent mean ± s.e.m., and each experiment was replicated at least twice on independent samples. Group comparisons were evaluated with two-way ANOVA followed by Bonferroni's post hoc tests; **p<0.01, ***p<0.001, ****p<0.0001.

Fgf2 induces GSK3β phosphorylation and prevents β-Catenin dissociation from tight junctions.

To further gain mechanistic insights, the molecular mechanisms underlying rescue of TNF-α-induced Cldn5 loss by Fgf2 were investigated. An integral part of TNF-α response in endothelial cells is activation of the Akt/ERK pathways which slow and eventually terminate the inflammatory signaling cascade[48]. Fgf2 is a potent activator of these pathways[49], and we evaluated whether the protective effects of Fgf2 on endothelial cells could be a result of rapid resolution of inflammatory signaling. Akt phosphorylates GSK3β serine residues inhibiting this redox sensitive enzyme and crucial mediator of TNF-α signaling known to disrupt tight junction integrity when activated in endothelial cells[50-52]. Therefore, we performed western blotting to assess the effects of TNF-α and Fgf2 on phosphorylation of GSK3β in the human HBEC-5i cell line (**Supp.Fig.5**). We found that 1h pretreatment with FGF2 induced GSK3β serine-9 phosphorylation (**Fig.4A**, *p=0.0332) but it did not prevent the rapid (5 min) dephosphorylation response upon TNF-α stimulation (**Fig.4A**). β-catenin is a downstream target of GSK3β which normally interacts with cadherins to promote tight junction integrity, but in the context of stress and inflammation it can be internalized to promote deleterious signaling[38,53,54]. In concordance with GSK3β inhibition, 1h of FGF2 treatment tended to reduce serine/threonine β-catenin phosphorylation (**Fig.4B**, p=0.0747). However, while TNF-α treatment initially reduced β-catenin phosphorylation (**p=0.0031), when co-administered with Fgf2 it led to a strong increase in β-catenin phosphorylation peaking 1h following TNF-α introduction (***p=0.0004) (**Fig.4B**). These results suggest that FGF2 can regulate β-catenin dynamics during inflammatory activation of brain endothelial cells which could mitigate stress-induced BBB alterations (**Fig.4C**).

With endothelial β-catenin signaling essential for tight junction regulation and BBB integrity, we assessed if changes in inflammation-induced β-catenin phosphorylation mediated by FGF2 treatment could affect β-catenin cellular distribution and tight junction morphology. β-catenin was stained by immunofluorescence in human HBEC-5i cells in control conditions or following 30 min of TNF-α treatment with or without FGF2. TNF-α-treated cells displayed tight junction spikes and discontinuities indicative of ultrastructural disruption as well as possible β-catenin internalization, whereas this morphology was not observed in control or TNF-α/FGF2 co-treated cells (**Fig.4D-E**). Furthermore, TNF-α induced distension of β-catenin labelled tight junction strands compared to vehicle-treated wells, as the width of β-catenin labelled tight junctions, was increased in TNF-α-treated wells (**Fig.4D-E**). This diffusion was normalized when cells were co-administered FGF2, suggesting a role for this growth factor in stabilizing β-catenin at sites of cell adhesion and preserving normal tight junction morphology. Since both Fgf2 and β-

299 catenin have been implicated in vascular remodeling and wound repair[55,56], a scratch wound test
300 was performed to evaluate endothelial healing responses after TNF-α treatment (**Fig.4F**). As
301 expected, TNF-α substantially reduced wound healing (**Fig.4F**). Interestingly, while FGF2 alone
302 did not affect wound repair compared to control, it did improve TNF-α-related reduction in healing
303 rate to result in a higher percentage of total healed area after 12 h (**Fig.4F**). This finding suggests
304 that this growth factor not only attenuates TNF-α-induced inflammatory signaling in endothelial
305 cells, but it can restore functional and healing properties of the BBB which may underlie beneficial
306 impact of EE in preventing stress-induced neurovascular alterations and promoting resilience.

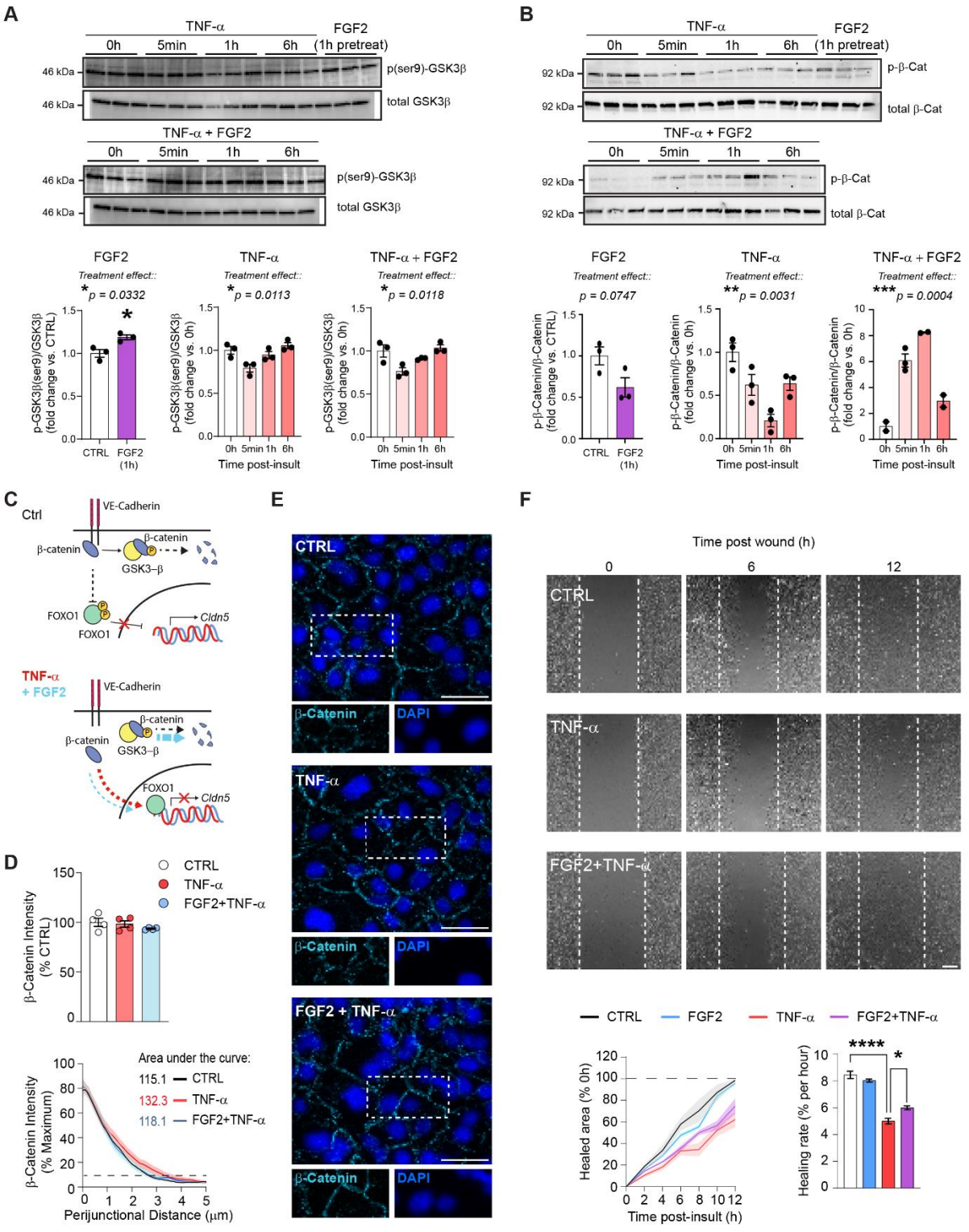

Figure 4. Fgf2 induces GSK3β phosphorylation and prevents β-Catenin dissociation from tight-junctions. A, 1 h pretreatment with Fgf2 increases serine-9 phosphorylation of GSK3β in HBEC-5i. TNF-α treatment induces rapid, transient dephosphorylation of GSK3β, but this effect is not reversed by Fgf2 coadministration. **B,** 1 h Fgf2 pretreatment diminishes basal β-catenin phosphorylation. Further, while TNF-α induces a rapid reduction in phosphorylated β-catenin, Fgf2 reverses this dynamic upon inflammatory activation. **C,** In health control endothelial

cells (top), β-catenin interacts with VE-Cadherin at the cell membrane, and this complex inhibits *Cldn5* transcriptional suppression by FOXO1. Excess cytosolic β-catenin is phosphorylated by GSK3β, targeting it for degradation. When stimulated with TNFα, unbound β-catenin complexes with FOXO1, leading to suppression of *Cldn5* expression (bottom, red arrow), while a small amount is targeted for degradation. Meanwhile, when FGF2 is co-administered with TNF-α (bottom, blue arrow), our results suggest that unbound β-catenin is strongly redirected toward GSK3β-mediated phosphorylation. **D,** 30 min of TNF-α is sufficient to induce β-catenin distribution at tight junctions with representative images on the right (**E**). **F,** Fgf2 attenuates TNF-α-induced reductions in the wound healing capacity of HBEC-5i. Data represent mean ± s.e.m., and each experiment was replicated at least twice on independent samples. Group comparisons were evaluated with one or two-way ANOVA followed by Bonferroni's post hoc tests or t-tests with Welch's correction when appropriate; *p<0.05, **p<0.01, ***p<0.001, ****p<0.0001.

Voluntary physical exercise protects the blood-brain barrier from deleterious effects of stress with light-cycle running promoting resilience.

Fgf2 is sensitive to environmental conditions, and modifiable lifestyle factors such as physical exercise (PE) have been linked to elevated expression of this growth factor in the brain[57]. Voluntary PE has been proposed as a critical variable for disease prevention and stress resilience associated with environmental enrichment experiments[58]. PE has benefits for neurovascular health, however it is unknown if it could protect from chronic stress-induced BBB alterations. After running wheel habituation, male mice were then randomly assigned to either control or stress groups which both had free voluntary access to running wheels in their home cage throughout the CSDS protocol (**Fig.5A**). Access to voluntary physical exercise during stress exposure increased the proportion of RES mice after CSDS to 53.6% (**Fig.5B),** and like EE (**Fig.1C**), strongly reduced social avoidance as measured by the time spent in the corners during the social interaction test (**Fig.5C**, ****p<0.0001 and **Supp.Fig.5A** for additional behavioral data). As expected, mice ran mostly during the dark cycle with distance increasing throughout the 10-d CSDS paradigm for the stressed mice to reach a total distance significant effect when compared to unstressed controls (**Fig.5D-E**, *p=0.0241). Intriguingly, RES mice ran more than other groups during the light cycle (**Fig.5F**, **p=0.0061) including right after the defeat bout (**Fig.5G**, ****p<0.0001 vs CTRL and *p=0.0136 vs SS), suggesting that PE may represent an active coping strategy when facing social stress.

Brains were collected 48h after the last stressor (**Fig.5A**) and BBB-related genes in the NAc and PFC analyzed and compared between groups. Few changes were noted between CSDS and control mice with access to PE, with the exception of a strong increase in *Cldn5* transcript levels in both the NAc (**p=0.005) and PFC (**p=0.0012) of stressed mice and this effect was driven by RES animals (**Fig.5H**, *p=0.0206 for NAc and *p=0.0233 for PFC). Conversely to our EE cohort where stressed mice displayed gene expression patterns distinct from controls, PCA analysis of the PE CSDS cohort revealed that CTRL, SS, and RES mice all form similar clusters, though stressed mice exhibit more variance (**Fig.5I** and **Supp.Fig.5E**). This implies that while EE alters more broadly the transcriptional stress response at the neurovasculature, PE more precisely targets *Cldn5* expression. At protein level, CSDS did not affect Cldn5 levels in the NAc of our PE cohort with all stressed mice exhibiting an increase in Fgf2 staining when compared to controls (**Fig.5J**). Altogether, our results indicate a protective effect of voluntary PE on stress-induced BBB changes in the male NAc dampening social avoidance and favoring resilience.

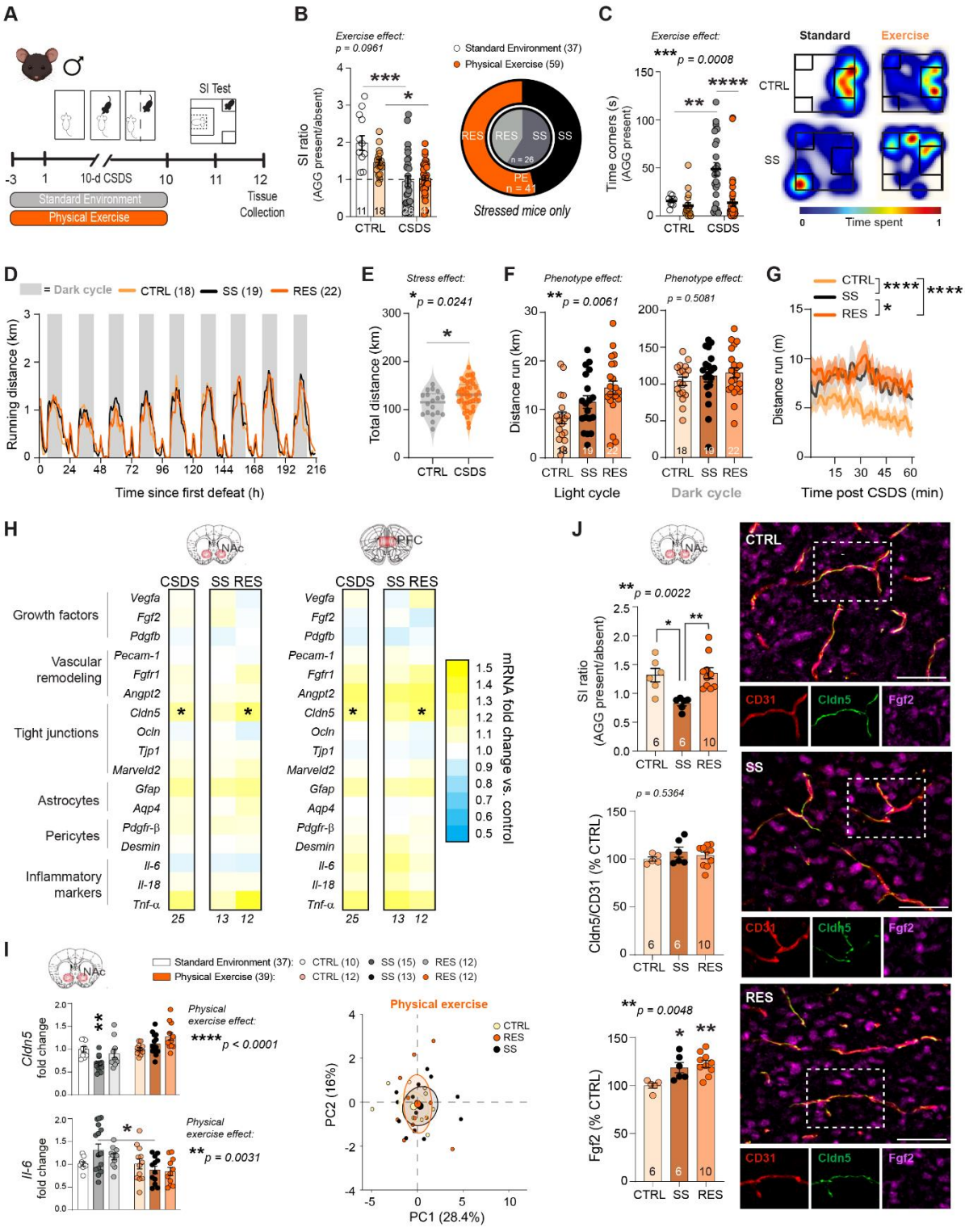

Figure 5. Physical exercise protects the blood-brain barrier from deleterious effects of stress with light-cycle running promoting resilience. A, Experimental timeline for chronic social defeat stress (CSDS) with physical exercise (PE). Male mice were habituated with a battery powered running wheel prior to CSDS and had voluntary access to wheel running until the last defeat, which was followed by social interaction (SI) testing. **B,** Compared to previously published results from CSDS with plain cages[9], stressed PE mice show similar deficits in social behavior

measured by the SI test, but a greater percentage of resilience. **C,** Stressed PE mice show substantially less time in corners of the SI test than those stressed in plain cages. Representative heatmaps of SI test in the second trial (aggressor present) show differences between CTRL and SS mice in CSDS with standard caging[9] and EE. **D,** Representative graph showing running activity per hour throughout CSDS. **E,** Stressed mice run slightly more than controls. **F,** Stress phenotype is associated with running during the light cycle, with RES mice running more during the day. **G**, RES mice run more in the hour following stress. **H,** Heatmaps showing transcription of BBB-related genes in the nucleus accumbens (NAc) and prefrontal cortex (PFC) after stress. Cldn5 is upregulated following 10 d CSDS in both brain regions of mice with access to PE.**I,** Increased Cldn5 expression and decreased Il-6 in SS EE mice compared to published data from SS mice in plain cages. **J,** No loss of Cldn5 immunofluorescent labelling in SS mice with PE access (scalebar = 50 μm). Fgf2 immunofluorescent labelling is increased in all stressed mice from the PE cohort. Data represent mean ± s.e.m., the number of animals is indicated on graphs. Group comparisons were evaluated with one- or two-way ANOVA followed by Bonferroni's post hoc tests, or t-tests with Welch's correction; *p<0.05, **p<0.01, ***p<0.001, ****p<0.0001.

Environment is a key factor determining BBB response to stress in mice and MDD pathogenesis in humans.

To this day, mood disorders including MDD are still diagnosed with questionnaires only. Identification of biomarkers with potential to inform clinicians for diagnosis and treatment choice is greatly needed and blood immune and vascular markers have received increasing attention in recent years[2,8,59-61]. To validate the importance of environmental conditions in stress-induced behavioral responses and underlying biology, we first conducted a hierarchical clustering analysis of all our mouse cohorts for BBB gene expression in stress sensitive brain areas. It revealed that environment is a key factor influencing BBB gene expression in both male (**Fig.6A**) and female (**Fig.6B**) mice. Indeed, groups tend to cluster by environmental conditions as opposed to stress exposure or phenotype. With this in mind, we explored if circulating FGF2 could be associated with human MDD when considering socioeconomic factors. Clinical evidence and postmortem studies related to FGF2 in the context of MDD are inconsistent[62-68] and this could be due to sampling heterogeneity. Blood serum FGF2 level was measured by ELISA in samples from men and women with a diagnosis of MDD and compared to matched controls. Sex and MDD severity of symptoms had a significant impact on FGF2 level (**Fig.6C**, **p=0.0036) which may explain previously reported discrepancies. In our cohort, having a university diploma and speaking more than one language at home was associated with lower depression rates (**Fig.6D**) so we tested the impact on FGF2 blood level. No difference was noted for income or employment status (data not shown). In individuals with no university diploma, an increase in circulating FGF2 was measured for MDD samples, an effect driven by men (**Fig.6E**, *p=0.020). Blood level of FGF2 was lower in men with MDD and a university diploma when compared to men without one (**Fig.6E**) however, it was significantly correlated with multiple symptoms of this psychiatric condition (**Fig.6F**, right). Importantly, a change in circulating FGF2 was associated with MDD in all men as assessed by the overall Patient Health Questionnaire (PHQ-9) score, a widely used screen test for depression (**Fig.6F**, right). Sex-specific symptomatology was noted with men with MDD reporting depressed mood, insomnia, and suicidal ideations while women mentioned anhedonia, fatigue, a change in appetite, loss of self-esteem and concentration capacities, all correlated with changes in blood FGF2 (**Fig.6F**). To sum up, circulating FGF2 may represent a promising blood biomarker of mood disorders, however, it is highly influenced by MDD severity, symptomatology, sex, environmental and socioeconomic factors.

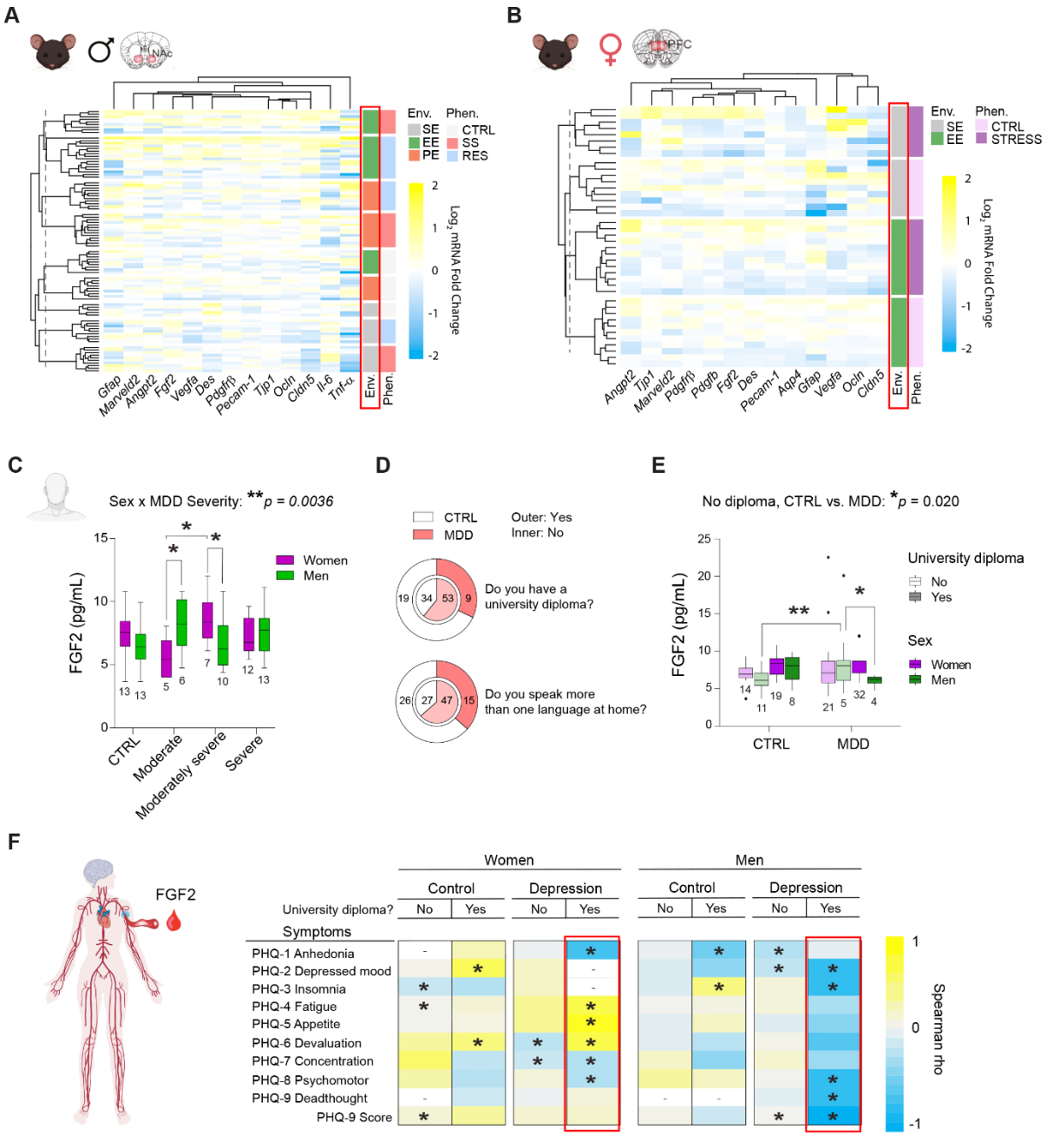

Figure 6. Environment is a key variable determining BBB response to stress and FGF2 a biomarker of MDD severity and symptomatology. Hierarchical clustering performed with euclidian distances of blood-brain barrier (BBB)-related gene expression changes induced by stress exposure in the male nucleus accumbens (**A**, NAc) or female prefrontal cortex (**B**, PFC) in standard conditions, with access to an enriched environment (EE), or voluntary physical exercise (PE). **C,** Fibroblast growth factor 2 (FGF2) level in blood serum samples from men and women with a diagnosis of major depressive disorder (MDD) at various degree of severity. **D,** Proportion of individuals in each group with a university diploma (top) or speaking more than one language at home (bottom). **E,** FGF2 blood level vs MDD diagnosis, sex, and education level. **F,** Spearman correlation between circulating FGF2 and MDD symptoms according to the Patient Health Questionnaire (PHQ-9) item constructs. Data represent mean ± s.e.m., the number of individuals is indicated on graphs. Group comparisons were evaluated with two-way ANOVA followed by Bonferroni's post hoc tests; *p<0.05, **p<0.01.

Discussion

Identifying, creating, and sustaining stimulating environments is a crucial strategy to ease the immense burden of mood disorders worldwide[69]. Environmental factors like socioeconomic status and physical exercise are negatively associated with MDD risk in humans[24,25], while access to complex housing or running wheels have been highlighted as protective strategies against maladaptive stress responses in mice[26]. Enrichment elicits changes in synaptic plasticity, growth of new neurons, and epigenetic modifications in neuronal populations[70], however the mechanisms linking environmental features to brain biology are complex, and their impact on non-neuronal cells is not well understood. The BBB is a crucial interface for communication between the environment and the brain, and disruption of this barrier is implicated in pathogenesis of stress-related mood disorders including depression[8,9]. Here, we demonstrate that housing conditions modify the neurovascular response to stress and influences social, anxiety- and depressive-like behavior in both male and female mice. Access to structural or physical enrichment during CSDS attenuated stress-induced loss of *Cldn5* gene expression and tight junction coverage of blood vessels in the male NAc, a brain region involved in emotional regulation and mood disorder pathophysiology. Further, we report that protective effects of home cage enrichment on the neurovasculature in male, but not female mice coincide with elevated Fgf2, a ubiquitous growth factor known to have anxiolytic and antidepressant effects[33-37], in the NAc. To see whether this increase could protect the BBB, we employed *in vitro* models and show that Fgf2 treatment attenuates downregulation of *Cldn5* expression and preserves endothelial monolayer integrity upon treatment with TNF-α in both mouse and human brain endothelial cells. Beneficial effect of Fgf2 on the brain vasculature when facing a chronic social stress challenge was confirmed with voluntary physical exercise, known to increase production of this growth factor. Finally, we found an association for circulating FGF2 level with depression severity and symptomatology in human blood samples from men and women with a diagnosis of MDD with an impact of socioeconomic factors in line with our mouse findings.

Previous studies have reported protective effects of complex environment or physical activity on the BBB in a variety of disease models including vascular dementia, multiple sclerosis, and Alzheimer's disease[71-74], but to our knowledge this is the first evidence that EE or PE can protect BBB properties against a purely psychological stressor. In males, EE was associated with a broad reconfiguration of stress-induced transcriptional patterns at the BBB, including upregulation of *Fgf2* growth factor expression, which is associated with maintenance of blood vessel integrity and maintenance of Cldn5 expression[32,75], and appears to drive EE-mediated change in *Cldn5* in response to stress. In previous RNA-seq comparisons of endothelial cell transcription from male mice after CSDS, SS and RES mice shared very few overlapping changes in gene expression[38], while the subset of transcripts assessed from our EE cohort showed SS and RES mice had many differentially expressed genes in common. These changes imply that instead of simply preventing stress-related damage in males, EE actively reconfigures the BBB transcriptional response to CSDS, which was confirmed by comparing the clustering of CTRL, SS, and RES mice based on transcription of BBB-related genes in standard CSDS or with access to EE. Similarly, access to PE during chronic stress also resulted in upregulation of *Cldn5* mRNA expression along with Fgf2 protein staining in the male NAc. However, instead of broadly altering the transcriptional response to stress, PE more precisely targets upregulation of *Cldn5* mRNA expression in stressed mice. These findings correspond with several lines of evidence suggesting that exercise and enrichment exert distinct effects on the brain and body[70,76,77]. Furthermore, it has

been argued that exercise is a crucial factor for the beneficial effects of environmental enrichment[58], and our results suggest this could be due to specific upregulation of *Cldn5* at the BBB to protect against damage.

The use of different stress protocols in each sex means we could not directly compare the effectiveness of environmental interventions between males and females. This study aimed to investigate the effects of environment on stress resilience, and thus requires a strong stress effect for which a rescue can be assessed. In female mice, CSDS is less applicable as females in the wild do not experience social aggression in the same way as males, and CD1 aggressors are moreover less likely to attack female intruders[40]. Several attempts have been made to overcome these barriers by chemogenetically inducing aggression in CD1s, or applying male urine to the back of female mice, in order to provoke an attack, but these methods still only succeed in producing stress-susceptible behaviors in about 1/3 of the stress cohort[8,41]. This suggests a ceiling for susceptibility and a potential barrier for detecting pro-resilient effects of enrichment. Thus, we opted to use instead a chronic variable stress protocol, which is well validated and produces strong behavioral alterations in female mice that correspond, to some extent, to human depression[42,78]. While direct comparisons of behavior and gene expression were not possible, we were still able to compare general patterns of change in BBB related genes between males and females and found strong sex differences in the BBB response to stress under standard versus enriched environment. In female mice, EE prevented SCVS-induced *Cldn5* loss in the PFC, but not in the NAc. SCVS reduces *Cldn5* expression in both PFC and NAc, but neurovascular disruption in the PFC alone is sufficient to promote depression-like behaviors in female mice[8]. Further, in contrast to males, EE did not promote an alternative transcriptional stress response in the female BBB but instead, stressed EE females maintained control-like gene expression. Clustering with PCA revealed that stressed males and females with EE access have distinct patterns of BBB transcriptional alterations. A possible explanation for sex differences in environment-BBB interactions during stress is that sex-specific steroid hormones are known to influence neurovascular unit function, potentially representing a controlling factor for determining the magnitude of impact from environmental change[43]. To better discern the relationship between sex, environment, and stress, a common stress paradigm for both sexes could enable direct comparisons of protective mechanisms in future studies.

The discovery of upregulated *Fgf2* gene and protein expression strictly in the male NAc after stress supports a sex-specific protective mechanism. Further, it suggests a common pathway associated with both EE and PE, implying that these conditions activate convergent biology in the brain to improve Cldn5 expression and BBB integrity. As mentioned above, Fgf2 has been shown to exert protective effects on endothelial cells and blood vessels, which could be related to the pro-resilient effects of stimulating environments. Also known as Fgf-basic or b-Fgf, Fgf2 belongs to the fibroblast growth factor family of proteins which stimulate tissue growth and development in a variety of organ systems. It is produced in several variants, with the main secreted version being a low molecular weight 18 kDa isoform[79]. Fgf2 exerts its biological functions through four Fgf receptors (FGFRs), namely FGFR1, FGFR2, FGFR3, and FGFR4, with FGFR1 being the most highly expressed on endothelial cells[80]. Studies have linked Fgf2 signaling to a variety of beneficial effects, showing for example that new blood vessels induced by Fgf2 show fewer fenestrations and less barrier leakage than vessels induced by vascular endothelial growth factors (VEGFs)[31]. Inhibition of FGFR1 in endothelial cells leads to endothelial permeability and loss of tight junction protein expression[32]. Moreover, in both astrocytes and microglia, Fgf2 treatment is sufficient to diminish pro-inflammatory activation and cytokine release upon insult *in vitro*[81,82]. On the other

hand, Fgf2 has been widely associated with anti-depressant and anxiolytic effects in rodents[33-37]. All this evidence suggests that increase of Fgf2 during stress in male EE and PE cohorts could be an adaptive response to protect against CSDS-induced tight junction loss and BBB permeability.

Next, we probed further into the role of Fgf2 at the BBB in the context of inflammatory damage to show how it may exert protective effects in endothelial cells in chronic social stress and MDD, both associated with elevated levels of circulating inflammatory cytokines[2,59,61,83]. As a simple model of stress-induced inflammation mouse and human brain endothelial cells were treated with TNF-α, a proinflammatory cytokine increased in the blood of humans with MDD and associated with circulating markers of vascular damage[44-46]. In addition, transcriptional pathways linked to TNF-α receptor signaling are upregulated in stress-susceptible mice[38]. Interestingly, vascular damage associated with TNF-α in a learned helplessness model of depression is gated by GSK3β which displays higher activity in learned helpless animals[10], corroborating *in vitro* findings that GSK3β mediates TNF-α-induced upregulation of leukocyte adhesion molecules on the brain endothelial cells[51]. Cldn5 plays an important functional role in the brain as the main tight junction protein regulating BBB permeability[84,85], and loss of this protein is observed in postmortem samples of humans with MDD[9,18,38]. Using our *in vitro* model, we found that Fgf2 protects against TNF-α-related loss of *Cldn5* expression in endothelial cells, suggesting a role as a protective agent at the BBB. In both mouse and human cells, Fgf2 attenuated *Cldn5* loss with significant rescue apparent after 6h of TNF-α treatment. Thus, rather than preventing initial *Cldn5* suppression, Fgf2 may engage slower-onset mechanisms which result in an early termination of inflammatory signaling. Intriguingly, the degree of *Cldn5* loss was more pronounced in HBEC-5i versus bEnd.3 suggesting that the mouse cells were more resistant to inflammation. This corresponds to longer term effects on endothelial monolayer integrity with chronic treatment, where TNF-α induced a stronger loss of TEER in HBEC-5i than bEnd.3. However, in both species inflammatory damage does increase barrier permeability, and this is prevented by Fgf2 treatment in both cases. Furthermore, after 7 days of TNF-α treatment, bEnd.3 cells stained for Cldn5 show a large number of membrane spikes and discontinuities, which are typically associated with stress or strain on cell membranes[47]. Spike morphology results from dysregulation of Cldn5 at the tight junction interface, leading to increased paracellular leakage; further, these spikes have been identified as 'hot spots' of vesicular transport and potentially play a role in compromising selectivity of influx to the brain[47,86]. Reduced spike morphology in cells co-treated with TNF-α and Fgf2 therefore indicates a stabilization of Cldn5 at tight junctions which could be related to prevention of BBB permeabilization following inflammatory challenge.

Fgf2 is known to interact with the Wnt/β-catenin system[87], which is crucial for development of BBB properties and maintenance of TJ ultrastructure[88,89], suggesting a possible avenue for the protective effects of Fgf2 shown above. Dysregulation of β-catenin during CSDS is moreover a driver of epigenetic Cldn5 suppression[38], and we suspected Fgf2 may interfere with this process. TNF-α is a strong activator of GSK3β which is thought to phosphorylate β-catenin, targeting it for degradation, during inflammation; conversely, Fgf2 stimulation activates signaling through Akt, a strong inhibitor of GSK3β[49-51]. In the absence of inflammation, we confirmed that Fgf2 increases deactivating serine-9 phosphorylation of GSK3β which corresponded with reduced β-catenin phosphorylation. Surprisingly, however, we found that β-catenin is modulated independently of GSK3β during following TNF-α induction, where it is rapidly dephosphorylated despite activation of GSK3β. Furthermore, Fgf2 had no effect on TNF-α-induced GSK3β activation but completely reversed trends in β-catenin phosphorylation after TNF-α treatment. The

observed drop in β-catenin phosphorylation as a result of TNF-α stimulation has also been reported in epithelial cells[90], but the biological significance of reversing this effect remains unclear. It is possible that this change influences β-catenin cell distribution, as TNF-α has been shown to induce β-catenin translocation to the nucleus where it suppresses Cldn5 expression, playing a role BBB disruption[54,90]. We found that 30 min of TNF-α promoted β-catenin accumulation in the cytoplasm, this is possibly related to inhibition of the proteasome by TNF-α, and thus less degradation of cytosolic β-catenin (data not shown)[91]. Further experiments will be needed to determine the precise mechanisms governing these drastic shifts in β-catenin phosphorylation and distribution during inflammation both with and without Fgf2.

In endothelial cells, β-catenin plays an important role in maintaining cell-cell adhesions, binding to VE-cadherin and linking it to the actin cytoskeleton in a structure with implications for both tight junction stability and cell motility[92]. We show that just 30 min of TNF-α treatment results in diffusion of β-catenin staining from cell-cell contacts, suggesting this as an early step in inflammation-related disruption of the junctional structure. Distension of cadherin complexes is potentially indicative of disrupted interaction between tight junction architecture and the actin cytoskeleton, an effect which could ultimately be related to the development of Cldn5 spikes and barrier hyperpermeability after chronic inflammatory damage[54]. Further evidence of dysfunction in membrane-cytoskeleton communication following TNF-α stimulation is a strong reduction of wound healing rate indicative of a decline in cell motility. β-catenin strongly regulates vascular cell growth and destabilization of this protein by TNF-α could be related to compromised repair mechanisms[56]. These connections are interesting but future experiments will be needed to confirm effects of TNF-α on actin dynamics at tight junctions as well as investigate causal relationships between this and changes to Cldn5 distribution and expression in the context of chronic stress exposure or mood disorders. Nevertheless, our results support TNF-α-induced dysfunction at sites of cell adhesion, and the fact the Fgf2 restores control-like β-catenin labelling as well as slightly rescuing wound healing rate demonstrates a stabilizing effect in the face of inflammatory damage.

Dysregulation of FGF signaling has been implicated in mood disorders, including MDD, and measurement of this growth factor as a brain and blood biomarker of psychiatric conditions has been considered yielding inconsistent results. Indeed, lower levels of FGF2 were reported in the dorsolateral PFC and anterior cingulate cortex[63] as well as hippocampus[93] of postmortem samples from depressed individuals however, no change was noted by others[64]. *FGF2* is mostly expressed by astrocytes in the brain but also other cell types[94,95]. Recent development and refining of single cell sequencing techniques shed light on the brain cellular heterogeneity including for glial cells and components of the neurovascular unit[3]. Taking advantage of these technologies may be useful to resolve these discrepancies in future work. Contradictory findings have also been reported for FGF2 blood serum or plasma level for individuals with psychiatric conditions when compared to matched healthy controls with decreased[96], increased[66-68,97], or no difference[65]. This could be due to heterogeneity of clinical aspects in the human cohorts such as comorbidities, treatments, symptoms, and lived experience. As reported here, socioeconomic factors may have an impact and should be carefully considered. To conclude, we investigated here BBB-related cellular and molecular mechanisms underlying resilience to stress and their promotion by an enriched environment, mimicking to some extent high socioeconomic status in humans, or physical exercise as an intervention to favor neurovascular health. We identified the growth factor Fgf2 as a promising target to protect the BBB when facing social adversity and argue that it could

598 represent an interesting biomarker to move towards personalized medicine and tailored treatment
599 in the context of mood disorders.

600

601 **Acknowledgements**

602 This research was supported by the Canadian Institutes for Health Research (CIHR, Project Grant
603 #427011 to C.M.), Fonds de recherche du Quebec – Santé (FRQS, Junior 2 salary award to C.M.)
604 and C.M. Sentinel North Research Chair funded by Canada First Research Excellence Fund.
605 S.E.J.P., J.L.S., L.D.A., L.B.B., K.A.D., and A.C. are supported by scholarships from CIHR,
606 FRQS, Réseau québécois sur le suicide, les troubles de l'humeur et les troubles associés (RQSHA),
607 and NeuroQuebec. The Signature Consortium acknowledges contributions to the Biobank
608 Signature of the CR-IUSMM (www.banquesignature.ca). The Biobank Signature received funding
609 from the Fondation de l'Institut Universitaire de Santé Mentale de Montréal, Bell cause pour la
610 cause, and the RQSHA. The authors would like to sincerely thank Dr. Jack McGugan from the
611 department of anaesthesiology and perioperative medicine at Queen's University, who performed
612 the 3D printing of our scratch wound template.

613 The authors also thank all the members of the Signature Consortium: Philippe Beauchamp-Kerr,
614 Felix-Antoine Berube, Janick Boissonneault, Francois Borgeat, Lionel Cailhol, Pierre David,
615 Simon Ducharme, Alexandre Dumais, Helen Findlay, Stéphane Guay, Steve Geoffrion, Charles-
616 Edouard Giguere, Roger Godbout, Alexandre Hudon, Robert-Paul Juster, Real Labelle, Marc
617 Lavoie, Myriam Lemyre, Alain Lesage, Cécile Le Page, Olivier Lipp, Sonia Lupien, Jean-Pierre
618 Melun, Marie-France Marin, Carolle Marullo, Francois Noel, Jean-Francois Pelletier, Vincent
619 Tascherau-Dumouchel, Pierrich Plusquellec, Stephane Potvin, , Ahmed-Jérome Romain, Marc
620 Sasseville, Daniel St-Laurent, Manuel Serrano, Emmanuel Stip, Christo Todorov, Valerie
621 Tourjman, Samir Taga, Claudia Trudel-Fitzgerald, Martha Francoise Ulysse, Andreas Ziegenhorn,
622 from the Institut Universitaire en Santé Mentale de Montréal, Centre Intégré Universitaire de Santé
623 Et Service Sociaux Est, Montréal, Québec, Canada.

624 **Author contributions**

625 S.E.J.P. and C.M. designed the research. S.E.J.P., J.L.S., A.C., E.R., F.C.R., L.D.A., L.B.B.,
626 K.A.D., A.C. and M.L. performed the research including behavioral experiments, molecular,
627 biochemical, and morphological analysis. The Signature Consortium contributed the human blood
628 samples and related demographic and sociodemographic data. S.E.J.P., J.L.S. and C.M. analyzed
629 the data and wrote the manuscript, which was edited by all authors.

630 **Declaration of interests**

631 The authors declare no competing interest.

632

633 **References**

634 1 Collaborators, G. B. D. M. D. Global, regional, and national burden of 12 mental
635 disorders in 204 countries and territories, 1990-2019: a systematic analysis for the Global

Burden of Disease Study 2019. *Lancet Psychiatry* **9**, 137-150 (2022). https://doi.org:10.1016/S2215-0366(21)00395-3

2 Hodes, G. E., Kana, V., Menard, C., Merad, M. & Russo, S. J. Neuroimmune mechanisms of depression. *Nat Neurosci* **18**, 1386-1393 (2015). https://doi.org:10.1038/nn.4113

3 Dion-Albert, L., Dudek, K. A., Russo, S. J., Campbell, M. & Menard, C. Neurovascular adaptations modulating cognition, mood, and stress responses. *Trends Neurosci* **46**, 276-292 (2023). https://doi.org:10.1016/j.tins.2023.01.005

4 Martin, L. A., Neighbors, H. W. & Griffith, D. M. The experience of symptoms of depression in men vs women: analysis of the National Comorbidity Survey Replication. *JAMA Psychiatry* **70**, 1100-1106 (2013). https://doi.org:10.1001/jamapsychiatry.2013.1985

5 Bangasser, D. A. & Cuarenta, A. Sex differences in anxiety and depression: circuits and mechanisms. *Nat Rev Neurosci* **22**, 674-684 (2021). https://doi.org:10.1038/s41583-021-00513-0

6 Labonte, B. *et al.* Sex-specific transcriptional signatures in human depression. *Nat Med* **23**, 1102-1111 (2017). https://doi.org:10.1038/nm.4386

7 Seney, M. L. *et al.* Opposite Molecular Signatures of Depression in Men and Women. *Biol Psychiatry* **84**, 18-27 (2018). https://doi.org:10.1016/j.biopsych.2018.01.017

8 Dion-Albert, L. *et al.* Vascular and blood-brain barrier-related changes underlie stress responses and resilience in female mice and depression in human tissue. *Nat Commun* **13**, 164 (2022). https://doi.org:10.1038/s41467-021-27604-x

9 Menard, C. *et al.* Social stress induces neurovascular pathology promoting depression. *Nat Neurosci* **20**, 1752-1760 (2017). https://doi.org:10.1038/s41593-017-0010-3

10 Cheng, Y. *et al.* TNFalpha disrupts blood brain barrier integrity to maintain prolonged depressive-like behavior in mice. *Brain Behav Immun* **69**, 556-567 (2018). https://doi.org:10.1016/j.bbi.2018.02.003

11 Lehmann, M. L., Poffenberger, C. N., Elkahloun, A. G. & Herkenham, M. Analysis of cerebrovascular dysfunction caused by chronic social defeat in mice. *Brain Behav Immun* **88**, 735-747 (2020). https://doi.org:10.1016/j.bbi.2020.05.030

12 Sawicki, C. M. *et al.* Social defeat promotes a reactive endothelium in a brain region-dependent manner with increased expression of key adhesion molecules, selectins and chemokines associated with the recruitment of myeloid cells to the brain. *Neuroscience* **302**, 151-164 (2015). https://doi.org:10.1016/j.neuroscience.2014.10.004

13 Daneman, R. & Prat, A. The blood-brain barrier. *Cold Spring Harb Perspect Biol* **7**, a020412 (2015). https://doi.org:10.1101/cshperspect.a020412

14 Kaplan, L., Chow, B. W. & Gu, C. Neuronal regulation of the blood-brain barrier and neurovascular coupling. *Nat Rev Neurosci* **21**, 416-432 (2020). https://doi.org:10.1038/s41583-020-0322-2

15 Segarra, M., Aburto, M. R. & Acker-Palmer, A. Blood-Brain Barrier Dynamics to Maintain Brain Homeostasis. *Trends Neurosci* **44**, 393-405 (2021). https://doi.org:10.1016/j.tins.2020.12.002

16 Niklasson, F. & Agren, H. Brain energy metabolism and blood-brain barrier permeability in depressive patients: analyses of creatine, creatinine, urate, and albumin in CSF and blood. *Biol Psychiatry* **19**, 1183-1206 (1984).

17 Futtrup, J. *et al.* Blood-brain barrier pathology in patients with severe mental disorders: a systematic review and meta-analysis of biomarkers in case-control studies. *Brain Behav Immun Health* **6**, 100102 (2020). https://doi.org:10.1016/j.bbih.2020.100102

18 Greene, C., Hanley, N. & Campbell, M. Blood-brain barrier associated tight junction disruption is a hallmark feature of major psychiatric disorders. *Transl Psychiatry* **10**, 373 (2020). https://doi.org:10.1038/s41398-020-01054-3

19 Kamintsky, L. *et al.* Blood-brain barrier imaging as a potential biomarker for bipolar disorder progression. *Neuroimage Clin* **26**, 102049 (2020). https://doi.org:10.1016/j.nicl.2019.102049

20 Diamond, M. C., Krech, D. & Rosenzweig, M. R. The Effects of an Enriched Environment on the Histology of the Rat Cerebral Cortex. *J Comp Neurol* **123**, 111-120 (1964). https://doi.org:10.1002/cne.901230110

21 Sirevaag, A. M., Black, J. E., Shafron, D. & Greenough, W. T. Direct evidence that complex experience increases capillary branching and surface area in visual cortex of young rats. *Brain Res* **471**, 299-304 (1988). https://doi.org:10.1016/0165-3806(88)90107-1

22 Ekstrand, J., Hellsten, J. & Tingstrom, A. Environmental enrichment, exercise and corticosterone affect endothelial cell proliferation in adult rat hippocampus and prefrontal cortex. *Neurosci Lett* **442**, 203-207 (2008). https://doi.org:10.1016/j.neulet.2008.06.085

23 Paton, S. E. J., Solano, J. L., Coulombe-Rozon, F., Lebel, M. & Menard, C. Barrier-environment interactions along the gut-brain axis and their influence on cognition and behaviour throughout the lifespan. *J Psychiatry Neurosci* **48**, E190-E208 (2023). https://doi.org:10.1503/jpn.220218

24 Lorant, V. *et al.* Socioeconomic inequalities in depression: a meta-analysis. *Am J Epidemiol* **157**, 98-112 (2003). https://doi.org:10.1093/aje/kwf182

25 Teychenne, M., Ball, K. & Salmon, J. Sedentary behavior and depression among adults: a review. *Int J Behav Med* **17**, 246-254 (2010). https://doi.org:10.1007/s12529-010-9075-z

26 Lehmann, M. L. & Herkenham, M. Environmental enrichment confers stress resiliency to social defeat through an infralimbic cortex-dependent neuroanatomical pathway. *J Neurosci* **31**, 6159-6173 (2011). https://doi.org:10.1523/JNEUROSCI.0577-11.2011

27 Mul, J. D. *et al.* Voluntary wheel running promotes resilience to chronic social defeat stress in mice: a role for nucleus accumbens DeltaFosB. *Neuropsychopharmacology* **43**, 1934-1942 (2018). https://doi.org:10.1038/s41386-018-0103-z

28 Cadoret, A. *et al.* Environmental conditions of recognition memory testing induce neurovascular changes in the hippocampus in a sex-specific manner in mice. *Behav Brain Res* **448**, 114443 (2023). https://doi.org:10.1016/j.bbr.2023.114443

29 Russo, S. J. & Nestler, E. J. The brain reward circuitry in mood disorders. *Nat Rev Neurosci* **14**, 609-625 (2013). https://doi.org:10.1038/nrn3381

30 Golden, S. A., Covington, H. E., 3rd, Berton, O. & Russo, S. J. A standardized protocol for repeated social defeat stress in mice. *Nat Protoc* **6**, 1183-1191 (2011). https://doi.org:10.1038/nprot.2011.361

31 Cao, R. *et al.* Comparative evaluation of FGF-2-, VEGF-A-, and VEGF-C-induced angiogenesis, lymphangiogenesis, vascular fenestrations, and permeability. *Circ Res* **94**, 664-670 (2004). https://doi.org:10.1161/01.RES.0000118600.91698.BB

32 Murakami, M. *et al.* The FGF system has a key role in regulating vascular integrity. *J Clin Invest* **118**, 3355-3366 (2008). https://doi.org:10.1172/JCI35298

33 Elsayed, M. *et al.* Antidepressant effects of fibroblast growth factor-2 in behavioral and cellular models of depression. *Biol Psychiatry* **72**, 258-265 (2012). https://doi.org:10.1016/j.biopsych.2012.03.003

34 Perez, J. A., Clinton, S. M., Turner, C. A., Watson, S. J. & Akil, H. A new role for FGF2 as an endogenous inhibitor of anxiety. *J Neurosci* **29**, 6379-6387 (2009). https://doi.org:10.1523/JNEUROSCI.4829-08.2009

35 Salmaso, N. *et al.* Fibroblast Growth Factor 2 Modulates Hypothalamic Pituitary Axis Activity and Anxiety Behavior Through Glucocorticoid Receptors. *Biol Psychiatry* **80**, 479-489 (2016). https://doi.org:10.1016/j.biopsych.2016.02.026

36 Simard, S. *et al.* Fibroblast growth factor 2 is necessary for the antidepressant effects of fluoxetine. *PLoS One* **13**, e0204980 (2018). https://doi.org:10.1371/journal.pone.0204980

37 Turner, C. A., Gula, E. L., Taylor, L. P., Watson, S. J. & Akil, H. Antidepressant-like effects of intracerebroventricular FGF2 in rats. *Brain Res* **1224**, 63-68 (2008). https://doi.org:10.1016/j.brainres.2008.05.088

38 Dudek, K. A. *et al.* Molecular adaptations of the blood-brain barrier promote stress resilience vs. depression. *Proc Natl Acad Sci U S A* **117**, 3326-3336 (2020). https://doi.org:10.1073/pnas.1914655117

39 Birey, F. *et al.* Genetic and Stress-Induced Loss of NG2 Glia Triggers Emergence of Depressive-like Behaviors through Reduced Secretion of FGF2. *Neuron* **88**, 941-956 (2015). https://doi.org:10.1016/j.neuron.2015.10.046

40 Lopez, J. & Bagot, R. C. Defining Valid Chronic Stress Models for Depression With Female Rodents. *Biol Psychiatry* **90**, 226-235 (2021). https://doi.org:10.1016/j.biopsych.2021.03.010

41 Harris, A. Z. *et al.* A Novel Method for Chronic Social Defeat Stress in Female Mice. *Neuropsychopharmacology* **43**, 1276-1283 (2018). https://doi.org:10.1038/npp.2017.259

42 Johnson, A., Rainville, J. R., Rivero-Ballon, G. N., Dhimitri, K. & Hodes, G. E. Testing the Limits of Sex Differences Using Variable Stress. *Neuroscience* **454**, 72-84 (2021). https://doi.org:10.1016/j.neuroscience.2019.12.034

43 Dion-Albert, L. *et al.* Sex differences in the blood-brain barrier: Implications for mental health. *Front Neuroendocrinol* **65**, 100989 (2022). https://doi.org:10.1016/j.yfrne.2022.100989

44 Tuglu, C., Kara, S. H., Caliyurt, O., Vardar, E. & Abay, E. Increased serum tumor necrosis factor-alpha levels and treatment response in major depressive disorder. *Psychopharmacology (Berl)* **170**, 429-433 (2003). https://doi.org:10.1007/s00213-003-1566-z

45 Fan, N., Luo, Y., Ou, Y. & He, H. Altered serum levels of TNF-alpha, IL-6, and IL-18 in depressive disorder patients. *Hum Psychopharmacol* **32** (2017). https://doi.org:10.1002/hup.2588

46 Hochman, E. *et al.* Serum claudin-5 levels among patients with unipolar and bipolar depression in relation to the pro-inflammatory cytokine tumor necrosis factor-alpha levels. *Brain Behav Immun* **109**, 162-167 (2023). https://doi.org:10.1016/j.bbi.2023.01.015

47 Lynn, K. S., Peterson, R. J. & Koval, M. Ruffles and spikes: Control of tight junction morphology and permeability by claudins. *Biochim Biophys Acta Biomembr* **1862**, 183339 (2020). https://doi.org:10.1016/j.bbamem.2020.183339

48 Zhou, Z. *et al.* Role of NF-kappaB and PI 3-kinase/Akt in TNF-alpha-induced cytotoxicity in microvascular endothelial cells. *Am J Physiol Renal Physiol* **295**, F932-941 (2008). https://doi.org:10.1152/ajprenal.00066.2008

49 Katoh, M. & Katoh, M. Cross-talk of WNT and FGF signaling pathways at GSK3beta to regulate beta-catenin and SNAIL signaling cascades. *Cancer Biol Ther* **5**, 1059-1064 (2006). https://doi.org:10.4161/cbt.5.9.3151

50 Cross, D. A., Alessi, D. R., Cohen, P., Andjelkovich, M. & Hemmings, B. A. Inhibition of glycogen synthase kinase-3 by insulin mediated by protein kinase B. *Nature* **378**, 785-789 (1995). https://doi.org:10.1038/378785a0

51 Eto, M., Kouroedov, A., Cosentino, F. & Luscher, T. F. Glycogen synthase kinase-3 mediates endothelial cell activation by tumor necrosis factor-alpha. *Circulation* **112**, 1316-1322 (2005). https://doi.org:10.1161/CIRCULATIONAHA.105.564112

52 Ramirez, S. H. *et al.* Inhibition of glycogen synthase kinase 3beta promotes tight junction stability in brain endothelial cells by half-life extension of occludin and claudin-5. *PLoS One* **8**, e55972 (2013). https://doi.org:10.1371/journal.pone.0055972

53 Hoffmeister, L., Diekmann, M., Brand, K. & Huber, R. GSK3: A Kinase Balancing Promotion and Resolution of Inflammation. *Cells* **9** (2020). https://doi.org:10.3390/cells9040820

54 Taddei, A. *et al.* Endothelial adherens junctions control tight junctions by VE-cadherin-mediated upregulation of claudin-5. *Nat Cell Biol* **10**, 923-934 (2008). https://doi.org:10.1038/ncb1752

55 Oladipupo, S. S. *et al.* Endothelial cell FGF signaling is required for injury response but not for vascular homeostasis. *Proc Natl Acad Sci U S A* **111**, 13379-13384 (2014). https://doi.org:10.1073/pnas.1324235111

56 Salehi, A. *et al.* Up-regulation of Wnt/beta-catenin expression is accompanied with vascular repair after traumatic brain injury. *J Cereb Blood Flow Metab* **38**, 274-289 (2018). https://doi.org:10.1177/0271678X17744124

57 Gomez-Pinilla, F., Dao, L. & So, V. Physical exercise induces FGF-2 and its mRNA in the hippocampus. *Brain Res* **764**, 1-8 (1997). https://doi.org:10.1016/s0006-8993(97)00375-2

58 Rogers, J. *et al.* Dissociating the therapeutic effects of environmental enrichment and exercise in a mouse model of anxiety with cognitive impairment. *Transl Psychiatry* **6**, e794 (2016). https://doi.org:10.1038/tp.2016.52

59 Hodes, G. E., Menard, C. & Russo, S. J. Integrating Interleukin-6 into depression diagnosis and treatment. *Neurobiol Stress* **4**, 15-22 (2016). https://doi.org:10.1016/j.ynstr.2016.03.003

60 Osimo, E. F. *et al.* Inflammatory markers in depression: A meta-analysis of mean differences and variability in 5,166 patients and 5,083 controls. *Brain Behav Immun* **87**, 901-909 (2020). https://doi.org:10.1016/j.bbi.2020.02.010

61 Doney, E., Cadoret, A., Dion-Albert, L., Lebel, M. & Menard, C. Inflammation-driven brain and gut barrier dysfunction in stress and mood disorders. *Eur J Neurosci* **55**, 2851-2894 (2022). https://doi.org:10.1111/ejn.15239

62 Deng, Z., Deng, S., Zhang, M. R. & Tang, M. M. Fibroblast Growth Factors in Depression. *Front Pharmacol* **10**, 60 (2019). https://doi.org:10.3389/fphar.2019.00060

63 Evans, S. J. *et al.* Dysregulation of the fibroblast growth factor system in major depression. *Proc Natl Acad Sci U S A* **101**, 15506-15511 (2004). https://doi.org:10.1073/pnas.0406788101

64 Goswami, D. B. *et al.* Gene expression analysis of novel genes in the prefrontal cortex of major depressive disorder subjects. *Prog Neuropsychopharmacol Biol Psychiatry* **43**, 126-133 (2013). https://doi.org:10.1016/j.pnpbp.2012.12.010

65 Takebayashi, M., Hashimoto, R., Hisaoka, K., Tsuchioka, M. & Kunugi, H. Plasma levels of vascular endothelial growth factor and fibroblast growth factor 2 in patients with major depressive disorders. *J Neural Transm (Vienna)* **117**, 1119-1122 (2010). https://doi.org:10.1007/s00702-010-0452-1

66 Kahl, K. G. *et al.* Angiogenic factors in patients with current major depressive disorder comorbid with borderline personality disorder. *Psychoneuroendocrinology* **34**, 353-357 (2009). https://doi.org:10.1016/j.psyneuen.2008.09.016

67 Lu, S. *et al.* Elevated specific peripheral cytokines found in major depressive disorder patients with childhood trauma exposure: a cytokine antibody array analysis. *Compr Psychiatry* **54**, 953-961 (2013). https://doi.org:10.1016/j.comppsych.2013.03.026

68 Wu, C. K., Tseng, P. T., Chen, Y. W., Tu, K. Y. & Lin, P. Y. Significantly higher peripheral fibroblast growth factor-2 levels in patients with major depressive disorder: A preliminary meta-analysis under MOOSE guidelines. *Medicine (Baltimore)* **95**, e4563 (2016). https://doi.org:10.1097/MD.0000000000004563

69 Collins, P. Y. *et al.* Grand challenges in global mental health. *Nature* **475**, 27-30 (2011). https://doi.org:10.1038/475027a

70 van Praag, H., Kempermann, G. & Gage, F. H. Neural consequences of environmental enrichment. *Nat Rev Neurosci* **1**, 191-198 (2000). https://doi.org:10.1038/35044558

71 Leardini-Tristao, M. *et al.* Physical exercise promotes astrocyte coverage of microvessels in a model of chronic cerebral hypoperfusion. *J Neuroinflammation* **17**, 117 (2020). https://doi.org:10.1186/s12974-020-01771-y

72 Malkiewicz, M. A. *et al.* Blood-brain barrier permeability and physical exercise. *J Neuroinflammation* **16**, 15 (2019). https://doi.org:10.1186/s12974-019-1403-x

73 Qu, C. *et al.* Protection of blood-brain barrier as a potential mechanism for enriched environments to improve cognitive impairment caused by chronic cerebral hypoperfusion. *Behav Brain Res* **379**, 112385 (2020). https://doi.org:10.1016/j.bbr.2019.112385

74 Souza, P. S. *et al.* Physical Exercise Attenuates Experimental Autoimmune Encephalomyelitis by Inhibiting Peripheral Immune Response and Blood-Brain Barrier Disruption. *Mol Neurobiol* **54**, 4723-4737 (2017). https://doi.org:10.1007/s12035-016-0014-0

75 Bendfeldt, K., Radojevic, V., Kapfhammer, J. & Nitsch, C. Basic fibroblast growth factor modulates density of blood vessels and preserves tight junctions in organotypic cortical cultures of mice: a new in vitro model of the blood-brain barrier. *J Neurosci* **27**, 3260-3267 (2007). https://doi.org:10.1523/JNEUROSCI.4033-06.2007

76 Olson, A. K., Eadie, B. D., Ernst, C. & Christie, B. R. Environmental enrichment and voluntary exercise massively increase neurogenesis in the adult hippocampus via dissociable pathways. *Hippocampus* **16**, 250-260 (2006). https://doi.org:10.1002/hipo.20157

77 Viola, G. G. *et al.* Morphological changes in hippocampal astrocytes induced by environmental enrichment in mice. *Brain Res* **1274**, 47-54 (2009). https://doi.org:10.1016/j.brainres.2009.04.007

78 Hodes, G. E. *et al.* Sex Differences in Nucleus Accumbens Transcriptome Profiles Associated with Susceptibility versus Resilience to Subchronic Variable Stress. *J Neurosci* **35**, 16362-16376 (2015). https://doi.org:10.1523/JNEUROSCI.1392-15.2015

79 Bikfalvi, A., Klein, S., Pintucci, G. & Rifkin, D. B. Biological roles of fibroblast growth factor-2. *Endocr Rev* **18**, 26-45 (1997). https://doi.org:10.1210/edrv.18.1.0292

80 Yang, X. *et al.* Fibroblast growth factor signaling in the vasculature. *Curr Atheroscler Rep* **17**, 509 (2015). https://doi.org:10.1007/s11883-015-0509-6

81 Liddelow, S. A. *et al.* Neurotoxic reactive astrocytes are induced by activated microglia. *Nature* **541**, 481-487 (2017). https://doi.org:10.1038/nature21029

82 Tang, M. M., Lin, W. J., Pan, Y. Q. & Li, Y. C. Fibroblast Growth Factor 2 Modulates Hippocampal Microglia Activation in a Neuroinflammation Induced Model of Depression. *Front Cell Neurosci* **12**, 255 (2018). https://doi.org:10.3389/fncel.2018.00255

83 Hodes, G. E. *et al.* Individual differences in the peripheral immune system promote resilience versus susceptibility to social stress. *Proc Natl Acad Sci U S A* **111**, 16136-16141 (2014). https://doi.org:10.1073/pnas.1415191111

84 Hashimoto, Y., Greene, C., Munnich, A. & Campbell, M. The CLDN5 gene at the blood-brain barrier in health and disease. *Fluids Barriers CNS* **20**, 22 (2023). https://doi.org:10.1186/s12987-023-00424-5

85 Nitta, T. *et al.* Size-selective loosening of the blood-brain barrier in claudin-5-deficient mice. *J Cell Biol* **161**, 653-660 (2003). https://doi.org:10.1083/jcb.200302070

86 Schlingmann, B. *et al.* Regulation of claudin/zonula occludens-1 complexes by hetero-claudin interactions. *Nat Commun* **7**, 12276 (2016). https://doi.org:10.1038/ncomms12276

87 Tang, D., He, Y., Li, W. & Li, H. Wnt/beta-catenin interacts with the FGF pathway to promote proliferation and regenerative cell proliferation in the zebrafish lateral line neuromast. *Exp Mol Med* **51**, 1-16 (2019). https://doi.org:10.1038/s12276-019-0247-x

88 Hussain, B. *et al.* Endothelial beta-Catenin Deficiency Causes Blood-Brain Barrier Breakdown via Enhancing the Paracellular and Transcellular Permeability. *Front Mol Neurosci* **15**, 895429 (2022). https://doi.org:10.3389/fnmol.2022.895429

89 Liebner, S. *et al.* Wnt/beta-catenin signaling controls development of the blood-brain barrier. *J Cell Biol* **183**, 409-417 (2008). https://doi.org:10.1083/jcb.200806024

90 Jang, J. *et al.* WNT/beta-catenin pathway modulates the TNF-alpha-induced inflammatory response in bronchial epithelial cells. *Biochem Biophys Res Commun* **484**, 442-449 (2017). https://doi.org:10.1016/j.bbrc.2017.01.156

91 Shim, S. M. *et al.* Role of S5b/PSMD5 in proteasome inhibition caused by TNF-alpha/NFkappaB in higher eukaryotes. *Cell Rep* **2**, 603-615 (2012). https://doi.org:10.1016/j.celrep.2012.07.013

92 Hartsock, A. & Nelson, W. J. Adherens and tight junctions: structure, function and connections to the actin cytoskeleton. *Biochim Biophys Acta* **1778**, 660-669 (2008). https://doi.org:10.1016/j.bbamem.2007.07.012

93 Gaughran, F., Payne, J., Sedgwick, P. M., Cotter, D. & Berry, M. Hippocampal FGF-2 and FGFR1 mRNA expression in major depression, schizophrenia and bipolar disorder. *Brain Res Bull* **70**, 221-227 (2006). https://doi.org:10.1016/j.brainresbull.2006.04.008

94 Zhang, Y. *et al.* An RNA-sequencing transcriptome and splicing database of glia, neurons, and vascular cells of the cerebral cortex. *J Neurosci* **34**, 11929-11947 (2014). https://doi.org:10.1523/JNEUROSCI.1860-14.2014

95 Zhang, Y. *et al.* Purification and Characterization of Progenitor and Mature Human Astrocytes Reveals Transcriptional and Functional Differences with Mouse. *Neuron* **89**, 37-53 (2016). https://doi.org:10.1016/j.neuron.2015.11.013

96 He, S. *et al.* Decreased serum fibroblast growth factor - 2 levels in pre- and post-treatment patients with major depressive disorder. *Neurosci Lett* **579**, 168-172 (2014). https://doi.org:10.1016/j.neulet.2014.07.035

97 Liu, X. *et al.* Elevated serum levels of FGF-2, NGF and IGF-1 in patients with manic episode of bipolar disorder. *Psychiatry Res* **218**, 54-60 (2014). https://doi.org:10.1016/j.psychres.2014.03.042

Additional references related to Methods

98 Livak, K. J. & Schmittgen, T. D. Analysis of relative gene expression data using real-time quantitative PCR and the 2(-Delta Delta C(T)) Method. *Methods* **25**, 402-408 (2001). https://doi.org:10.1006/meth.2001.1262

99 Schindelin, J. *et al.* Fiji: an open-source platform for biological-image analysis. *Nat Methods* **9**, 676-682 (2012). https://doi.org:10.1038/nmeth.2019

100 Mosmann, T. Rapid colorimetric assay for cellular growth and survival: application to proliferation and cytotoxicity assays. *J Immunol Methods* **65**, 55-63 (1983). https://doi.org:10.1016/0022-1759(83)90303-4

101 Gassmann, M., Grenacher, B., Rohde, B. & Vogel, J. Quantifying Western blots: pitfalls of densitometry. *Electrophoresis* **30**, 1845-1855 (2009). https://doi.org:10.1002/elps.200800720

102 Pillai-Kastoori, L., Schutz-Geschwender, A. R. & Harford, J. A. A systematic approach to quantitative Western blot analysis. *Anal Biochem* **593**, 113608 (2020). https://doi.org:10.1016/j.ab.2020.113608

103 Suarez-Arnedo, A. *et al.* An image J plugin for the high throughput image analysis of in vitro scratch wound healing assays. *PLoS One* **15**, e0232565 (2020). https://doi.org:10.1371/journal.pone.0232565

104 Kroenke, K., Spitzer, R. L. & Williams, J. B. The PHQ-9: validity of a brief depression severity measure. *J Gen Intern Med* **16**, 606-613 (2001). https://doi.org:10.1046/j.1525-1497.2001.016009606.x

Methods.

Animals. Male and female C57BL/6 mice aged 8 weeks of age at arrival (Charles River Laboratories, Québec, Canada) were used for all experiments. Retired male CD-1 breeders were used as resident aggressors (AGG) for social defeat and social interaction tests. All mice were group housed in 27 × 21 × 14 cm polypropylene cages upon their arrival and left undisturbed for at least three days prior to experimentation. Mice were maintained on a 12-h light–dark cycle

(lights on from 0800 to 2000 h) with constant temperature, humidity (22 °C, 63%) and free access to water and food (Teklad Irradiated Laboratory Animal Diet, Madison, USA). All experimental procedures were approved by the animal care and use committee of Université Laval (2022-1061-1) and met the guidelines set out by the Canadian Council on Animal Care.

Housing conditions. Control and stressed EE mice were housed in a standard cage supplemented with a plastic house, nesting material, and a small plastic toy. When animals were moved between cages during CSDS, they maintained their original enrichment materials. Control and stress animals in the PE cohorts were housed in standard cages and habituated with battery powered, wireless running wheels (Med Associates) for five days prior the beginning of CSDS. This habituation period is based on previous reports as well as our observations (not shown) that running activity per day reaches a plateau after five days. Each animal was assigned a wheel which it was kept with throughout cage changes during the 10 d CSDS protocol. Data was collected and exported at 1-minute intervals using Wheel Manager software (Med Associates).

Chronic social defeat stress (CSDS). Male C57/Bl6 mice underwent CSDS as previously described[30]. AGG mice underwent three days of screening for aggression profile and were conditioned in social defeat cages separated halfway by a clear, perforated divider for 24 h prior to experiments. Experimental mice were subject to physical interaction with a novel CD-1 for five minutes a day over 10 consecutive days and subsequently housed in defeat cages opposite the CD-1 with the divider preventing physical altercation but allowing sensory contact. Interactions were stopped before the five-minute period elapsed if attacks were repeated and severe, or if wounding occurred. Unstressed controls were co-housed in social defeat cages on each side of a divider and were moved every other day. After the last bout of interaction, the experimental mice were single housed in standard cages for 24 h before undergoing a social interaction (SI) test, and tissue was collected 24 hours after that (**Fig.1A**).

Chronic variable stress (CVS). Female C57/Bl6 mice were housed in groups of four in standard cages for 6d CVS protocol as previously described[8]. Briefly, stressed mice were subject to three different alternating stressors, one per day, in the following order: 100 random mild foot shocks (0.45 mA) for 1 h, tail suspension for 1 h, and tube restraint within home cage for 1 h. Unstressed controls were handled every day. After the last stressor, mice were single housed for behavioral testing and tissue was collected 24 hours after the last test (**Fig.2A**).

Social interaction (SI) test. SI tests to assess social preference was performed under red light conditions as previously described[9,30]. Mice were placed in an open field arena with a small wire cage at one end for 150 s. Mice were then removed and the arena was cleaned, a CD-1 (AGG) was placed in the wire cage, and experimental mice were again allowed 150 s to freely explore the arena. Behavior in presence and absence of social target was tracked with AnyMaze software. Interaction zone (IZ) is defined as the area around the mesh cage. SI ratio was calculated by dividing the time in interaction zone in presence vs. absence of AGG. Mice with SI < 1 were classified as stress-susceptible (SS), while SI = 1 or > 1 were resilient (RES).

Elevated plus maze (EPM). The EPM apparatus is a cross-shaped plexiglass arena with 4 arms (12 cm width x 50 cm length) 1 m above ground level, where two arms had tall black walls (closed arms) and two were unprotected (open arms). Under red light, mice were placed in the middle of the maze and allowed to explore for 300 s. Behavior was automatically tracked (AnyMaze 6.1, Stoelting Co.). Time in closed arms is taken as a measure of anxiety-like behavior.

Sucrose preference test. Water bottles in standard cages were replaced with two 50 mL conical tubes containing water for a 48-h habituation. Next, water from one of the tubes was replaced with 1 % sucrose and mice were allowed to drink *ad libitum*. Tubes were switched after 24 h to account for place bias, and weights were recorded at 0 h, 24 h, and 48 h. Sucrose preference after 24 h was calculated by dividing weight of sucrose consumed by total weight of liquid.

Forced swim test (FST). Forced swim is used to evaluate learned helplessness as a measure of depression. Mice were placed in a 4 L glass beaker filled with 3 L lukewarm water under bright light for 360 s. Video of each session was manually evaluated for time spent immobile, defined as no movement or small hind-leg gestures needed to stay afloat, by blinded observers.

Cell culture. The human brain microvascular endothelial cell line HBEC-5i (ATCC CRL-3245) and mouse brain endothelial cell line bEnd.3 (ATCC CRL-2299) were subcultured and stored in banks at -150 ^{o}C. Cells were thawed as needed and cultured in DMEM/F12 supplemented with 10% fetal bovine serum, 25 ug/mL gentamicin (Gibco), and 1X endothelial cell growth supplement (ScienCell). Culture surfaces were precoated with 0.1% gelatin and cells were passaged when confluent (3-5 days) by washing with PBS, detaching with TrpLE Dissociation Reagent (Gibco), and seeding on gelatin coated flasks at desired concentration. Cells were used for experiments between passages 3 and 7, seeded at a density of 5 x 10^4 cells/cm^2. For immunofluorescence, cells were grown on gelatin coated 12mm glass coverslips (Marienfeld) which were previously hydrophilized by 10 min treatment with 0.1 M hydrochloric acid and sterilized for 10 min with 100% ethanol.

TNF-α and Fgf2 treatment. Human recombinant TNF-α and FGF2 (Gibco) were dissolved in sterile water per manufacturer's instructions and stored at -20 ^{o}C. Experiments were performed using HBEC-5i and bEnd.3 after 4-5 days *in vitro*. Cells were pretreated for 1 h with 10 ng/mL human recombinant FGF-2 (Gibco) or vehicle (sterile water). At the start of treatment, existing medium was completely aspirated and replaced with HBEC-5i cell culture medium containing either sterile water (vehicle), 10 ng/mL FGF2 + vehicle, vehicle + 10 ng/mL TNF-α, or 10 ng/mL FGF2 + 10 ng/mL TNF-α. Acute inflammation studies looked at the response to a single stimulus up to 24 h, while chronic inflammation was assessed by replacing the medium each day with fresh medium containing TNF-α and/or FGF2 over a period of up to 7 days.

Gene Expression Analysis. Mice were anesthetized by decapitation and brains were rapidly removed. 2.0 mm punches were taken from NAc and PFC in both hemispheres and frozen at -80 ^{o}C until use. HBEC-5i and bEnd.3 in a 6-well plate were pretreated for 1 h with Fgf2 or sterile water (vehicle) and then stimulated with TNF-α or TNF-α + FGF2 for 0 h (control), 1 h, 3 h, 6 h, or 24 h (3 wells/condition/timepoint). RNA was extracted from brain punches as well as HBEC-5i and bEnd.3 cells in 6-well plates using TRIzol (Invitrogen) homogenization and phase separation with chloroform. The clear RNA phase was processed further with the Pure Link RNA mini kit (Life Technologies) and assessed for purity and concentration with NanoDrop (Thermo Fisher Scientific). Complementary DNA (cDNA) was obtained with a reverse transcriptase reaction using Maxima-H-minus cDNA synthesis kit (Fisher Scientific). For qPRC reactions, each well of a 384-well plate contained 3 µL of sample cDNA, 1 µL qPCR primer (see **Table 1** for primer list), 5 µL Power up SYBR green (Fisher Scientific), and 1 µL distilled H_2O. In a thermocycler, samples were heated to 95 ^{o}C followed by 40 cycles of 95 ^{o}C for 15 s, 60 ^{o}C for 33 s and 72 ^{o}C for 33 s. Ct values were converted to normalized expression using the 2^{-ddCt} method[98] with *Gapdh* as the reference gene.

Immunofluorescent Staining. Whole brains of mice after rapid decapitation were flash frozen with isopentane on dry ice and stored at -80 °C until use. Frozen brains were embedded in OCT Compound (Thermo Fisher Scientific) and slices from PFC and NAc were collected using a cryostat (Leica) at 20 μm thickness. Brain slices and cells cultured on glass coverslips were post-fixed for 10 min in ice-cold methanol. After 3x5 min wash with PBS brain slices were incubated for 2 h in blocking solution (1% bovine serum albumin, 4% normal donkey serum, and 0.03% Triton X-100 in PBS) before overnight incubation with primary antibodies in blocking solution (see Table 2 for antibodies and dilutions). Samples were then washed 3x5 min with PBS and incubated with fluorophore-conjugated secondary antibodies in PBS, then washed again and stained with DAPI to visualize nuclei. Coverslips were mounted on slides using Prolong Diamond Antifade Mountant (Invitrogen). Z-stack images of the NAc and PFC were taken with at 20X (Z = 10 μm) and 40X (Z = 3 μm) on an epifluorescence microscope (Carl Zeiss).

Fluorescent image analysis. Analysis of brain tissue images was automatically performed in batches using Fiji ImageJ software[99]. For each channel, maximum intensity projection was performed and resulting images were processed with rolling ball background subtraction followed by noise removal of bright artefacts less than 2 μm. In Cd31 channel only, continuity of blood vessels was ensured by 2D Gaussian blur, σ = 2 μm. Processed images were binarized using automatic thresholding algorithms to measure positive staining area. β-catenin distribution at tight junctions in HBEC-5i cells was assessed by a blinded experimenter who sampled one tight junction from each quadrant of each image for a total of 48 TJs per condition. β-catenin distribution was assessed by measuring fluorescence intensity across a 10 μm line drawn perpendicular to the junction plane.

Cell viability assay. 3-(4,5-dimethyl-2-thiazolyl)-2,5-diphenyl-2H-tetrazolium (MTT) (Millipore Sigma) is converted to water-insoluble product formazan by reduction at mitochondrial complex II of the electron transport chain. This reaction can therefore act as a proxy for mitochondrial respiration and cell viability[100]. Briefly, cells in a 24-well plate were treated with 500 μM MTT and incubated (37°C and 5% CO2) for 2 h. Media was removed, and formazan crystals were dissolved in 500 μL dimethyl sulfoxide for absorbance readings at 570 nm using a spectrophotometer. Viability is calculated as a percent of control reading.

Trans-endothelial electrical resistance (TEER). For TEER studies, HBEC-5i were seeded on transwell polycarbonate culture inserts (Millicell) with 12 mm diameter and 3 μm pore size. TEER measurements were taken using the Millicell® ERS-2 Electrical Resistance System. Gelatin coated insert with no cells was used as a blank. Electrodes were habituated in complete growth media at room temp for 10 mins before reading resistance across cell monolayers. TEER was calculated as resistance of sample minus resistance of blank, multiplied by membrane surface area (0.6 cm^2). TEER measurements were normalized to baseline for each well and are presented as percentage of control; raw TEER values are available in **Supp.Fig.4**.

Protein extraction and western blot. HBEC-5i and bEnd.3 in a 6-well plate were pretreated for 1 h with Fgf2 or sterile water (vehicle) and then stimulated with TNF-α or TNF-α + FGF2 for 0 h (control), 5 min, 1 h, or 6 h (3 wells/condition/timepoint). Protein was extracted at desired timepoints by washing with ice-cold PBS and then lysing cells with 200 μL cell lysis buffer (Cell Signaling Cat. No. 9803) supplemented with protease inhibitor cocktail (Cell signalling Cat. No. 5871). Samples were sonicated in ice-cold water, centrifuged for 10 min (13 000 rpm, 4 °C), and

supernatant transferred to a new tube. Protein level was quantified using the Pierce™ BCA Protein Assay Kit (ThermoFisher Cat. No. 23250) per manufacturers instructions. Samples were diluted 1:10 and absorbance values were read on a spectrophotometer at 562 nm. Protein levels were calculated from standard curve. Samples were prepared for gel electrophoresis by adding a volume containing 20 ug protein to 3 uL 1 M DTT and 7.5 µL 4X Laemmli sample buffer (BioRad Cat. No. 1610747) and topping up to 30 µL with deionized water. Samples and protein ladder (10-250 kDa, Cell Signaling Cat. No. 74124) were pipetted into wells of a 18-well Criterion™ TGX Stain-Free™ pre-cast gel (4-15%, BioRad Cat. No. 5678084) and separated by SDS-PAGE. Protein was transferred to a polyvinylidene difluoride (PVDF) membrane with 60 min of 90 V current in transfer buffer (25 mM Tris base, 192 mM glycine, 20% methanol in deionized water). Membranes were blocked in Tris-buffered Saline (TBS) supplemented with 0.1% Tween (TBST) and 0.5% BSA and incubated overnight with primary antibodies in blocking solution at 4 °C (see **Table 2** for antibodies and dilutions). Membranes were washed 3x10 min in TBST and incubated 1 h with horseradish-peroxidase (HRP)-conjugated secondary antibodies in TBST. Membranes were washed again and signals on blots were revealed by enhanced chemiluminescence (ECL) reagents (BioRad Cat. No. 1705060) in a ChemiDoc imaging system (BioRad). Band intensity was estimated in Fiji ImageJ by removing background separately for each lane and measuring volume of the peak signal[101,102]. Phosphorylated GSK3β and β-Catenin levels were normalized to total GSK3β and β-Catenin. Total protein was measured with Stain-Free™ imaging technology and used as a loading control for Cldn5 levels.

Scratch Wound Assay. HBEC-5i in 24-well plates were pre-treated with Fgf2 for 1 h and subsequently stimulated with Fgf2, TNF-α, Fgf2 + TNF-α, or sterile H2O as vehicle (CTRL) for 24 h prior to wound induction. Scratch wound was induced using a sterile 200 µL pipette tip aligned with a custom 3D-printed plastic template to ensure all scratch sizes were equal, following the recommendations of previous publications[103]. Wounded cells were washed twice with DMEM/F12 and subsequently incubated with Fgf2, TNF-α, Fgf2 + TNF-α, or sterile H2O as vehicle. Images were taken at 5X on the brightfield setting of an epifluorescence microscope at 2 h intervals beginning immediately after scratch and continuing until 12 h. Wound size was manually evaluated using the Wound Healing Size Tool plugin for Fiji[103].

Human serum sample collection. All human blood samples were provided by the Signature Bank from the Centre de recherche de l'Institut universitaire en santé mentale de Montréal (CR-IUSMM) under approval of the institution's Ethics Committee. Samples from volunteers with major depressive disorder were collected at the emergency room of the Institut universitaire en santé mentale de Montréal of CIUSSS de l'Est-de-Montreal and samples from healthy volunteers at the CR-IUSMM. All donors provided informed consent and signed a 7-page document detailing the goals of the Signature Bank, participants involvement (questionnaires and tissue sampling), advantages vs risks, compensation, confidentiality measures, rights as participant and contact information. Subjects with known history of drug abuse were excluded. Demographic characteristics associated with each sample are listed in **Supp.Table 3**. Depressive behaviours were assessed by the Patient Health Questionnaire (PHQ-9), which scores each of the nine Diagnostic and Statistical Manual of Mental Disorders (DSM) IV criteria[104]. All experiments were performed under the approval of Université Laval and CERVO Brain Research Center Ethics Committee *Neurosciences et santé mentale (Project #2019-1540)*.

Enzyme-Linked Immunosorbent Assay (ELISA). Serum levels of Fgf2 were assessed with the Quantikine® Human FGF2 ELISA kit from R&D systems (Cat. No. DFB50), following manufacturers instructions. Serum samples were diluted 1:2 and absorbance read at 450 nm with wavelength correction at 570 nm on a VICTOR Nivo multimode plate reader. Concentration were calculated from a 4PL standard curve using MyAssays.com data analysis tool.

Statistical analysis. Statistical comparisons were performed using GraphPad Prism 9 software. Each dataset was tested for normality (Shapiro-Wilk test, alpha = 0.05) and outliers (Grubb's test, alpha = 0.05). Animals identified as outliers in two or more distinct behavioral measures were removed from further analysis. Two-group comparisons were performed using two-tailed unpaired Welch's t-test (normal distribution) or Mann-Whitney U-test (non-gaussian distribution). Multiple comparisons were assessed with one- and two-way analysis of variance (ANOVA) followed by Bonferroni post-hoc testing (normal distribution) or Kruskal-Wallis test with Dunn's post-hoc test (non-gaussian distribution). Principal component analysis (PCA) was performed using the R software, package FactoMineR, and missing values imputed with missMDA.

Data availability. All data supporting the findings of this study are available within the paper and Supplementary Information.

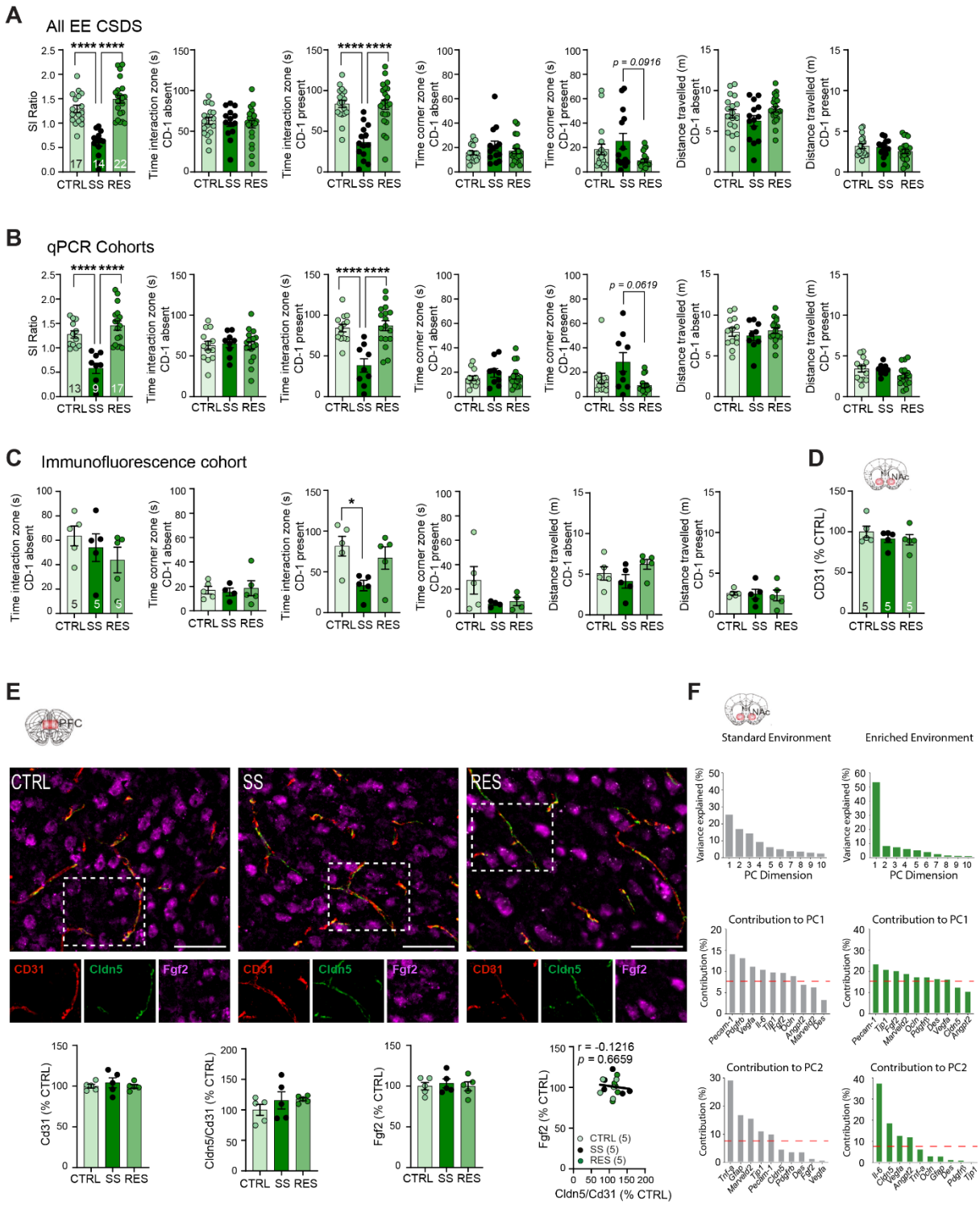

Supplementary Figure 1. Additional behavioral, morphological, and statistical data for male mice with access to an enriched environment. Additional behavioral metrics are shown from social interaction (SI) tests of male mice with enriched environment (EE) after CSDS for all cohorts grouped (**A**), and then split by tissue use, qPCR (**B**) and immunofluorescence (**C**). **D,** Staining for CD31, a blood vessel marker, in the male NAc is not affected by CSDS with EE access. **E**, No substantial changes are observed in immunofluorescent labelling of Cd31, Cldn5, or Fgf2 in male PFC after 10 d CSDS with EE. **F**, Contribution of principal component (PC) dimensions and genes involved in PC1

and PC2 as determined by principal component analysis (PCA) of qPCR datasets from male NAc following 10 d CSDS in standard environment (Menard et al., 2017) and EE. Data represent mean ± s.e.m., the number of animals is indicated on graphs. Group comparisons were evaluated with one- or two-way ANOVA followed by Bonferroni's posttests; *p<0.05, **p<0.01, ***p<0.001, ****p<0.0001.

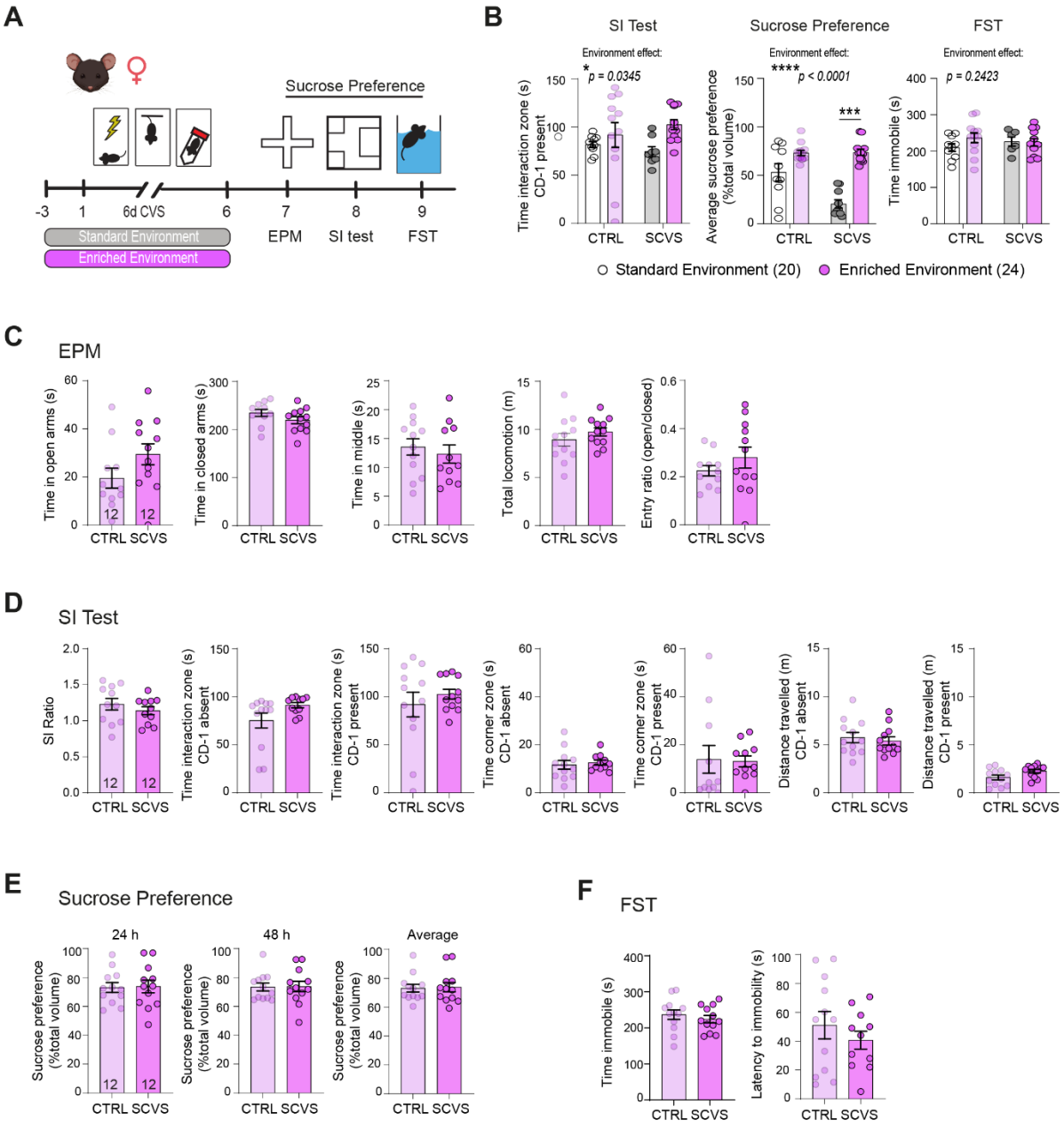

Supplementary Figure 2. Additional behavioral data for female mice with access to an enriched environment. **A,** Experimental timeline for assessing depressive and anxiety-like behavior after subchronic variable stress (SCVS) with enriched environment (EE). Female mice were housed with a nestlet, plastic chew toy, and shelter beginning 3 d prior to stress and continuing until the last session, followed by testing with elevated plus maze (EPM), social interaction (SI) tests, sucrose preference, and the forced swim test (FST). **B,** Compared to previously published findings (Dion-Albert, 2022), EE ameliorates SCVS-induced deficits in the SI test and sucrose preference. Additional behavioral metrics are presented for the EPM (**C**), SI test (**D**), sucrose preference test (**E**), and FST (**F**). Data represent mean ± s.e.m., the number of animals is indicated on graphs. Group comparisons were evaluated with one- or two-way ANOVA followed by Bonferroni's posttests, or t-test with Welch's correction where appropriate; *p<0.05, **p<0.01, ***p<0.001, ****p<0.0001.

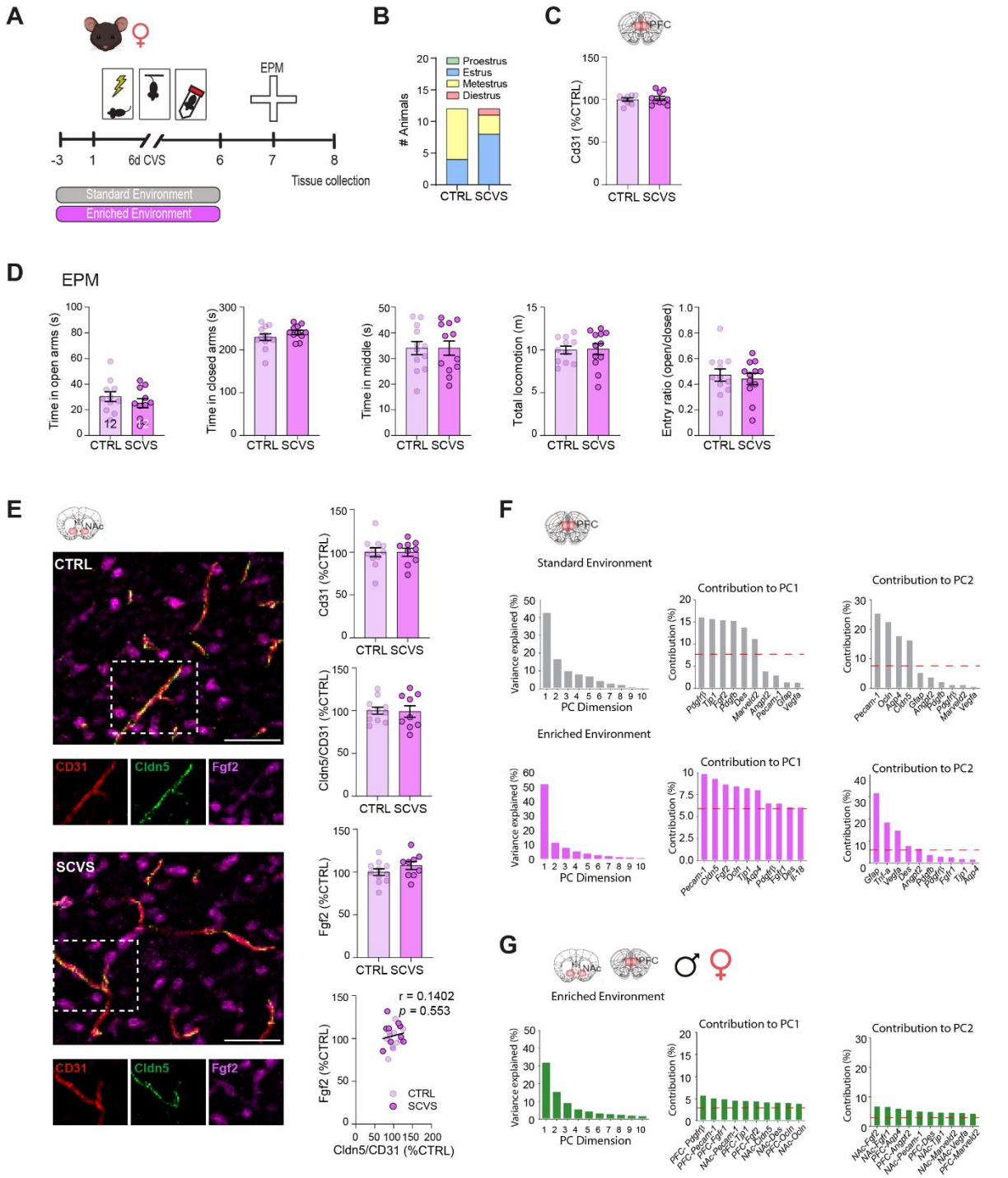

Supplementary Figure 3. Additional behavioral, morphological, and statistical data for female mice with access to an enriched environment. A, Experimental timeline for SCVS with access to enriched environment (EE), followed by EPM testing and tissue collection. Female mice were housed with a nestlet, plastic chew toy, and shelter beginning 3 d prior to stress and continuing until the last session. **B,** Estrus cycle stage determined at sacrifice in CTRL and SCVS groups. **C,** No change in Cd31 immunolabelling in the female PFC post-SCVS. **D,** Additional behavioral metrics from EPM testing of this cohort. **E,** No significant changes in Cd31, Cldn5, or Fgf2 immunolabelling in the female NAc following SCVS with EE. **F**, Contribution of principal component (PC) dimensions and genes involved

in PC1 and PC2 as determined by principal component analysis (PCA) of qPCR datasets from female NAc following SCVS in standard environment (Dion-Albert et al., 2022) and EE. **G,** Contribution of principal component (PC) dimensions and genes involved in PC1 and PC2 as determined by principal component analysis (PCA) of qPCR datasets from both NAc + PFC of males and females following SCVS with access to EE. Data represent mean ± s.e.m., the number of animals is indicated on graphs. Group comparisons were evaluated with t-test with Welch's correction where appropriate.

A

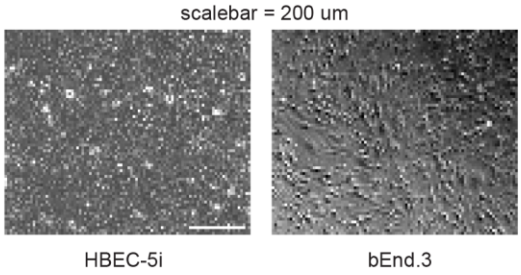

B

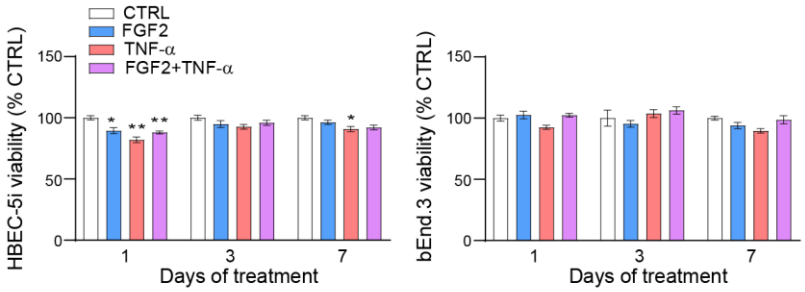

C

HBEC-5i (human)		Baseline		Day 1		Day 3		Day 7	
		Mean	St. Dev	Mean	St. Dev	Mean	St. Dev	Mean	St. Dev
TEER (Ω*cm^2)	CTRL (8)	36.825	8.32582	37.725	7.435	42.975	12.6262	41.625	12.2164
	FGF2 (8)	38.175	7.64979	38.25	6.40424	41.625	10.8945	43.425	11.0678
	TNFα (8)	39.225	8.24513	37.65	5.73486	38.325	10.0779	39.45	12.2618
	FGF2+TNFα (8)	39.225	8.81196	42	5.22084	43.725	10.6245	45.525	15.2783

bEnd.3 (mouse)		Baseline		Day 1		Day 3		Day 7	
		Mean	St. Dev	Mean	St. Dev	Mean	St. Dev	Mean	St. Dev
TEER (Ω*cm^2)	CTRL (8)	21.6	3.36367	22.875	4.11261	27	2.29035	28.35	1.99643
	FGF2 (8)	20.25	2.62025	22.425	4.74545	28.125	3.5632	29.475	3.62048
	TNFα (8)	22.725	1.71026	21.6	3.57131	25.8	2.44949	27.975	2.37712
	FGF2+TNFα (8)	22.875	2.74838	23.7	5.14143	28.425	4.7346	30.375	3.15764

Supplementary Figure 4. Additional morphological and cell viability data for HBEC human endothelial cells. **A,** Representative brightfield images of HBEC-5i and bEnd.3 cells demonstrating endothelial morphology, scalebar = 200 µm. **B,** HBEC-5i and bEnd.3 cell viability is not substantially altered by 7 d treatment with FGF2 and/or TNF-α. **C,** Raw TEER measurements for HBEC-5i and bEnd.3.

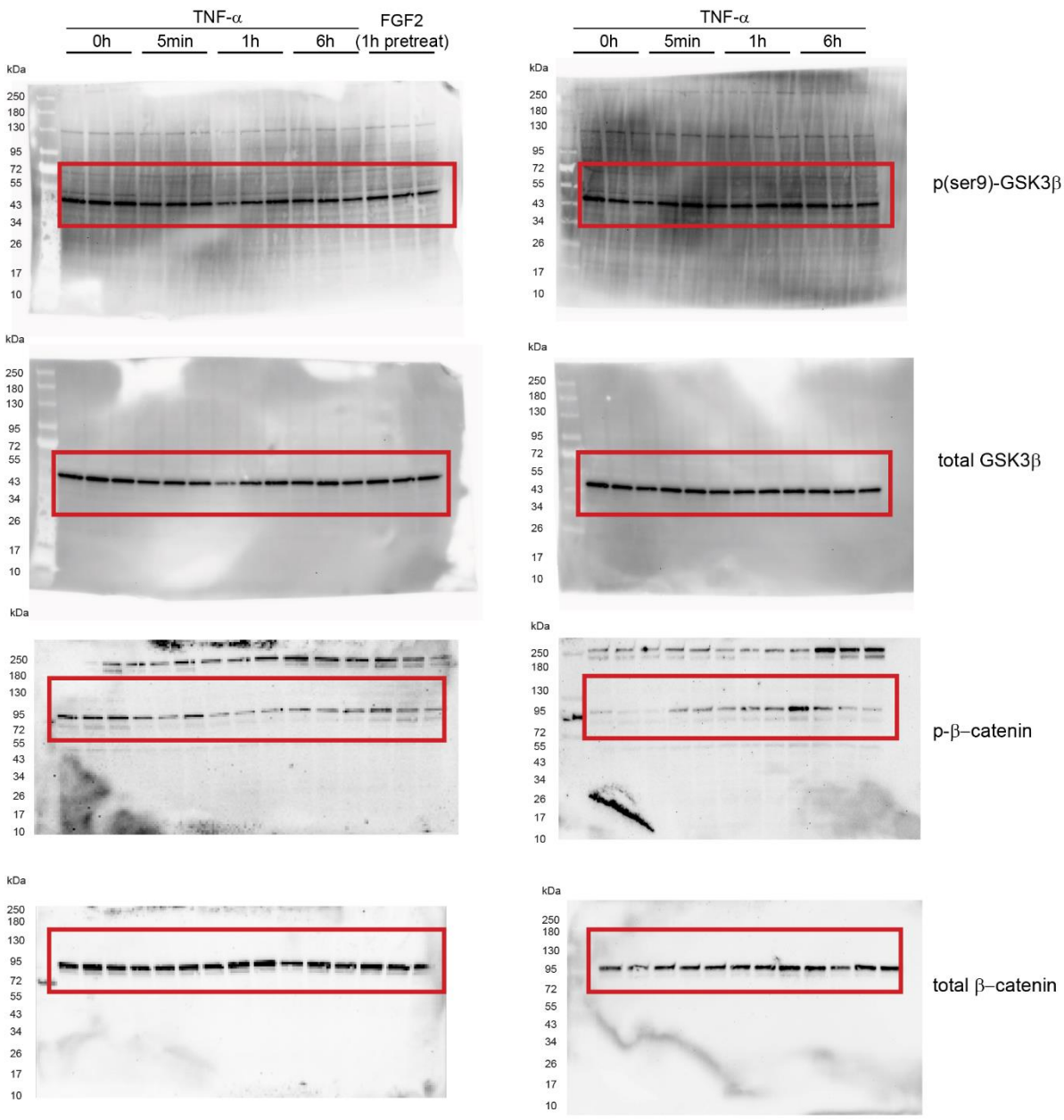

Supplementary Figure 5. Full-length Western Blots. Full-length Western blots of HBEC-5i cells treated with tumor necrosis factor alpha (TNF-α) or fibroblast growth factor 2 (FGF2). Protein levels were evaluated for glycogen synthase kinase-3 beta (GSK3β) serine 9 residue (p-ser9)-GSKβ, total GSK3β, phospho-beta-catenin (p-β-catenin) and finally, total β-catenin.

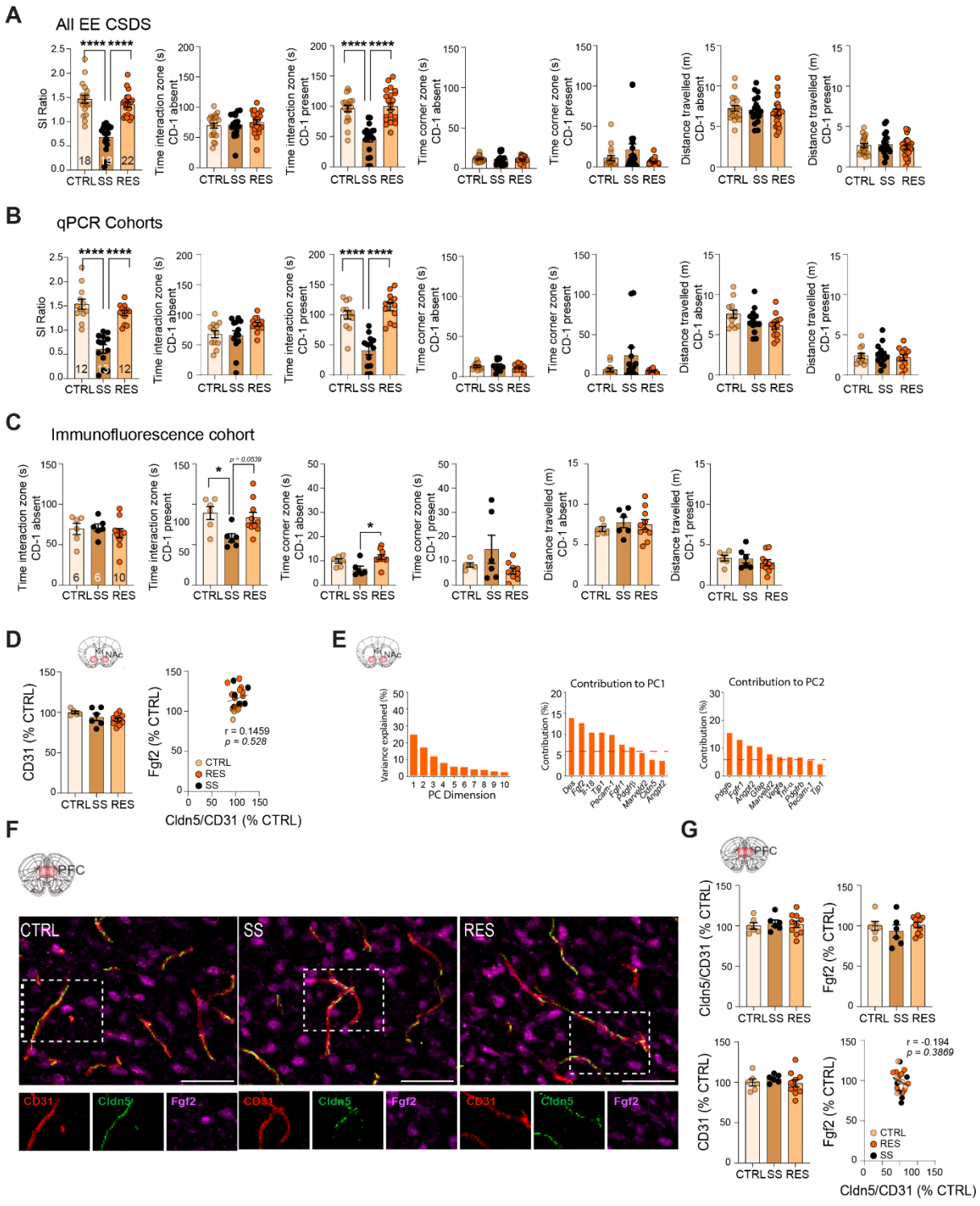

Supplementary Figure 6. Additional behavioral, morphological, and statistical data for male mice with access to physical exercise. Additional behavioral metrics are shown from social interaction (SI) tests of male mice with physical exercise (PE) after CSDS for all cohorts grouped (**A**), and then split by tissue use, qPCR (**B**) and immunofluorescence (**C**). **D,** Staining for CD31, a blood vessel marker, in the male NAc is not affected by CSDS with EE access, and Cldn5 levels do not correlate with Fgf2. **E**, Contribution of principal component (PC) dimensions and genes involved in PC1 and PC2 as determined by principal component analysis (PCA) of qPCR datasets from male

NAc following 10 d CSDS in standard environment (Menard et al., 2017) and EE. **F**, Representative immunofluorescent images of Cd31, Cldn5, and Fgf2 in male PFC after 10 d CSDS, scalebar = 50 μm, and **G,** No substantial changes are observed in immunofluorescent labelling of these markers. Data represent mean ± s.e.m., the number of animals is indicated on graphs. Group comparisons were evaluated with one- or two-way ANOVA followed by Bonferroni's posttests; *p<0.05, **p<0.01, ***p<0.001, ****p<0.0001.

1206 **Supplementary Table 1. Primers for RT-qPCR.**

Gene	Species	Ref Seq #	Assay ID	Forward Primer (5'-3')	Reverse Primer (5'-3')
Gapdh	Mouse	NM_008084(1)	Mm.PT.39a.1	PrimeTime® qPCR Primers Exon Location 2 - 3	
Vegfa	Mouse	NM_001025250(3)	Mm.PT.58.14200306	PrimeTime® qPCR Primers Exon Location 1 - 2	
Fgf2	Mouse	NM_008006(1)	Mm.PT.56a.5129235	PrimeTime® qPCR Primers Exon Location 1 - 3	
Pdgfb	Mouse	NM_011057(1)	Mm.PT.58.32585335	PrimeTime® qPCR Primers Exon Location 2 - 3	
Pecam-1	Mouse	NM_001032378(2)	Mm.PT.58.43167370	PrimeTime® qPCR Primers Exon Location 7 – 8	
Fgfr1	Mouse	NM_001079908(3)	Mm.PT.58.6948463	PrimeTime® qPCR Primers Exon Location 6 - 7	
Angpt2	Mouse	NM_007426(1)	Mm.PT.58.29139310	PrimeTime® qPCR Primers Exon Location 1a - 2	
Cldn5	Mouse	NM_013805(1)		TTTCTTCTATGCGCAGTTGG	GCAGTTTGGTGCCTACTTCA
Ocln	Mouse	NM_008756(1)	Mm.PT.58.42749240	PrimeTime® qPCR Primers Exon Location 7 - 9	
Tjp1	Mouse	NM_001163574(2)	Mm.PT.58.29459730	PrimeTime® qPCR Primers Exon Location 18 - 19	
Marveld2	Mouse	NM_001038602(2)	Mm.PT.58.7719303	PrimeTime® qPCR Primers Exon Location 5 - 7	
Gfap	Mouse	NM_010277(1)	Mm.PT.58.31297710	PrimeTime® qPCR Primers Exon Location 6 - 9	
Aqp4	Mouse	NM_009700(1)	Mm.PT.58.9080805	PrimeTime® qPCR Primers Exon Location 1 - 2	
Pdgfrb	Mouse	NM_001146268(2)	Mm.PT.56a.5869521	PrimeTime® qPCR Primers Exon Location 23 - 24	
Des	Mouse	NM_010043(1)	Mm.PT.58.13181631	PrimeTime® qPCR Primers Exon Location 7 - 9	
Il-6	Mouse	NM_031168.2		TAGTCCTTCCTACCCCAATTTCC	TTGGTCCTTAGCCACTCCTTC
Il-18	Mouse	NM_008360.2		GACTCTTGCGTCAACTTCAAGG	CAGGCTGTCTTTTGTCAACGA
Tnf-α	Mouse	NM_013693.3		CCCTCACACTCAGATCATCTTCT	GCTACGACGTGGGCTACAG
Vcam1	Mouse	NM_011693(1)	Mm.PT.58.9687546	PrimeTime® qPCR Primers Exon Location 5 - 6	
Ripk1	Mouse	NM_009068(1)	Mm.PT.58.7201430	PrimeTime® qPCR Primers Exon Location 4 - 5	
Hdac1	Mouse	NM_008228(1)	Mm.PT.58.14183463	PrimeTime® qPCR Primers Exon Location 7 - 8	
Foxo1	Mouse	NM_019739(1)	Mm.PT.58.6477586	PrimeTime® qPCR Primers Exon Location 1 - 2	
Gsk3β	Mouse	NM_019827(1)	Mm.PT.58.41280327	PrimeTime® qPCR Primers Exon Location 6 - 7	
GAPDH	Human	NM_002046(1)	Hs.PT.39a.22214836	PrimeTime® qPCR Primers Exon Location 2 - 3	
CLDN5	Human	NM_001130861(2)	Hs.PT.58.1483777.g	PrimeTime® qPCR Primers Exon Location 1 - 1[1]	
OCLN	Human	NM_001205254(3)	Hs.PT.58.15235048	PrimeTime® qPCR Primers Exon Location 6 - 7	
RIPK1	Human	NM_003804(1)	Hs.PT.58.15545621	PrimeTime® qPCR Primers Exon Location 7 - 8	
HDAC1	Human	NM_004964(1)	Hs.PT.58.38680914	PrimeTime® qPCR Primers Exon Location 3 - 4	
FOXO1	Human	NM_002015(1)	Hs.PT.58.40005627	PrimeTime® qPCR Primers Exon Location 1 - 2	
GSK3β	Human	NM_001146156(2)	Hs.PT.58.40111551	PrimeTime® qPCR Primers Exon Location 6 - 7	
FGFR1	Human	NM_001174067(1)	Hs.PT.58.15035470	PrimeTime® qPCR Primers Exon Location 3 - 4	
FGF2	Human	NM_002006(1)	Hs.PT.58.24613308	PrimeTime® qPCR Primers Exon Location 1 - 2	
VCAM-1	Human	NM_001199834(3)	Hs.PT.58.20405152	PrimeTime® qPCR Primers Exon Location 2a - 3	
IL-1β	Human	NM_000576(1)	Hs.PT.58.1518186	PrimeTime® qPCR Primers Exon Location 1 - 3	
IL-6	Human	NM_000600(1)	Hs.PT.58.40226675	PrimeTime® qPCR Primers Exon Location 4 - 5	

1207

1208

1209 **Supplementary Table 2. Primary and secondary antibodies**

Immunofluorescence				
Target	**Company**	**Cat #**	**Host**	**Dilution**
Cd31	Invtrogen	14-0311-85	Rat	1:100
Cldn5	Invitrogen	34-1600	Rabbit	1:250
Fgf2	Biosensis	10782-612	Sheep	1:200
Cy2 Anti-Rat	Jackson ImmunoResearch	712-175-153	Donkey	1:400
Cy3 Anti-Rabbit	Jackson ImmunoResearch	711-225-152	Donkey	1:400
Cy5 Anti-Sheep	Jackson ImmunoResearch	713-175-147	Donkey	1:400
Western Blot				
Target	**Company**	**Cat #**	**Host**	**Dilution**
p(ser9)-Gsk3β	Cell Signalling	9336	Rabbit	1:1000
Gsk3β	Cell Signalling	9315	Rabbit	1:1000
p-β-Catenin	Cell Signalling	9562	Rabbit	1:1000
β-Catenin	Cell Signalling	9561	Rabbit	1:1000
Cldn5	Invitrogen	34-1600	Rabbit	1:1000
Anti-Rabbit IgG, HRP	Cell Signalling	7074	Goat	1:5000

1210

1211

1212 **Supplementary Table 3. Demographic and sociodemographic data of the human cohort.**

Sex	Dx	Severity	> than 2 Languages	University	Employed	Income level
F	CTRL	Minimal	Yes	No	Yes	Below
F	CTRL	Minimal	No	Yes	No	Above
F	CTRL	Minimal	Yes	No	No	Below
F	CTRL	Minimal	No	Yes	Yes	Above
F	CTRL	Minimal	No	Yes	Yes	Above
F	CTRL	Minimal	No	No	No	Above
F	CTRL	Minimal	No	No	No	Below
M	CTRL	Minimal	No	No	No	Below
F	CTRL	Minimal	No	No	Yes	Above
F	CTRL	Minimal	Yes	Yes	Yes	Below
M	CTRL	Minimal	No	Yes	Yes	Above
F	CTRL	Mild	No	No	No	Below
F	CTRL	Minimal	Yes	No	Yes	Below
F	CTRL	Minimal	No	No	Yes	Below
F	CTRL	Minimal	No	Yes	Yes	Above
F	CTRL	Minimal	Yes	No	Yes	Above
M	CTRL	Minimal	No	No	No	Below
M	CTRL	Mild	No	Yes	Yes	Above
F	CTRL	Minimal	No	No	No	Below
M	CTRL	Minimal	Yes	No	No	Below
F	CTRL	Minimal	No	Yes	Yes	Above
F	CTRL	Minimal	Yes	No	Yes	Below
M	CTRL	Minimal	No	Yes	Yes	Below
M	CTRL	Minimal	No	No	No	Below
F	CTRL	Mild	Yes	Yes	No	Below
M	CTRL	Minimal	No	No	Yes	Below
M	CTRL	Minimal	No	No	No	Below
M	CTRL	Minimal	Yes	No	No	Below
F	CTRL	Minimal	Yes	No	Yes	Below
F	CTRL	Minimal	Yes	Yes	No	Below
F	CTRL	Minimal	Yes	No	N/A	N/A
M	CTRL	Minimal	Yes	No	Yes	Above
F	CTRL	Minimal	Yes	Yes	No	Below
F	CTRL	Minimal	No	Yes	No	Below
F	CTRL	Minimal	Yes	Yes	No	Below
M	CTRL	Minimal	No	No	Yes	Above
M	CTRL	Mild	Yes	Yes	No	Below
M	CTRL	Minimal	Yes	Yes	Yes	Above
F	CTRL	Minimal	Yes	No	Yes	Below

M	CTRL	Minimal	No	No	Yes	Above
M	CTRL	Minimal	Yes	No	Yes	Below
M	CTRL	Minimal	Yes	No	Yes	Above
M	CTRL	Minimal	No	No	Yes	Below
M	CTRL	Minimal	Yes	Yes	Yes	Above
M	CTRL	Minimal	No	Yes	Yes	Below
M	CTRL	Minimal	Yes	No	Yes	Below
M	CTRL	Minimal	Yes	No	Yes	Below
F	CTRL	Minimal	Yes	No	Yes	Below
M	CTRL	Minimal	No	No	No	Below
M	CTRL	Minimal	No	No	Yes	Above
M	CTRL	Minimal	No	No	Yes	Above
M	CTRL	Minimal	Yes	Yes	No	Above
M	CTRL	Minimal	Yes	No	No	Below
F	MDD	Moderately severe	Yes	No	No	Below
M	MDD	Severe	Yes	No	Yes	Below
M	MDD	Moderately severe	No	No	Yes	Below
M	MDD	Moderate	No	No	No	Above
M	MDD	Severe	No	No	Yes	Below
M	MDD	Moderately severe	No	No	No	Below
M	MDD	Severe	No	No	Yes	Above
F	MDD	Moderately severe	Yes	No	Yes	Below
F	MDD	Moderately severe	No	No	No	Below
M	MDD	Moderate	No	No	No	Below
F	MDD	Severe	No	No	No	Below
M	MDD	Severe	No	No	Yes	Below
M	MDD	Severe	No	No	No	Below
M	MDD	Severe	Yes	No	Yes	Above
F	MDD	Moderately severe	No	No	No	Below
M	MDD	Moderate	No	No	No	Below
M	MDD	Severe	No	No	No	Above
M	MDD	Moderate	No	No	Yes	Below
F	MDD	Severe	Yes	No	Yes	Below
M	MDD	Severe	No	No	Yes	Above
F	MDD	Moderate	No	Yes	Yes	Below
M	MDD	Moderately severe	No	No	No	N/A
F	MDD	Severe	No	No	Yes	Below

F	MDD	Moderately severe	No	No	Yes	Below
M	MDD	Severe	No	No	No	Below
M	MDD	Moderately severe	No	No	No	Below
F	MDD	Severe	No	Yes	Yes	Below
M	MDD	Severe	No	No	Yes	Above
M	MDD	Moderate	No	No	No	Above
F	MDD	Severe	No	No	Yes	N/A
M	MDD	Severe	Yes	No	No	Below
M	MDD	Moderate	Yes	No	No	Below
F	MDD	Severe	No	Yes	Yes	Above
F	MDD	Severe	Yes	No	No	Below
M	MDD	Severe	No	No	No	Below
F	MDD	Severe	No	No	Yes	Below
M	MDD	Severe	No	No	Yes	Above
F	MDD	Severe	No	No	No	Below
M	MDD	Severe	No	No	No	Below
M	MDD	Severe	No	No	Yes	Above
M	MDD	Severe	No	No	No	Below
F	MDD	Moderate	No	No	No	Below
M	MDD	Severe	Yes	No	No	N/A
F	MDD	Severe	No	No	Yes	Below
F	MDD	Moderate	Yes	No	No	Below
M	MDD	Moderately severe	No	No	Yes	Below
F	MDD	Moderately severe	No	No	Yes	Below
M	MDD	Moderately severe	No	No	Yes	Above
M	MDD	Moderately severe	No	No	Yes	Below
M	MDD	Moderately severe	No	Yes	Yes	Below
F	MDD	Moderately severe	No	No	Yes	Above
F	MDD	Moderate	No	No	Yes	Below
F	MDD	Severe	No	No	No	Below
F	MDD	Moderately severe	No	Yes	No	Below
M	MDD	Severe	No	No	No	Below
F	MDD	Severe	No	Yes	Yes	Above
M	MDD	Severe	No	Yes	Yes	Below
F	MDD	Moderate	Yes	No	No	Below

F	MDD	Severe	Yes	No	No	Below
M	MDD	Moderately severe	Yes	No	Yes	Above
M	MDD	Moderately severe	No	Yes	Yes	Below
M	MDD	Severe	Yes	No	No	Below
F	MDD	Severe	No	No	Yes	Above
M	MDD	Moderately severe	Yes	No	Yes	Below
M	MDD	Severe	Yes	Yes	No	Below

1213